Analysis of the energetic potential and mathematical modelling of the thermal decomposition of the palm kernel shell and empty fruit bunch of the African oil palm

Carlos Junior Arias Hernández, Julián Fernando Manrique Pinto

Trabajo de grado para optar al título de

Ingeniero Mecánico

Director

Yesid Javier Rueda Ordóñez, PhD.

Ingeniero Mecánico

Universidad Industrial de Santander

Facultad de Ingeniería Físico-Mecánicas

Escuela de Ingeniería Mecánica

Bucaramanga

2018

Contents

Tables

Figures

RESUMEN

TÍTULO: ANÁLISIS DEL POTENCIAL ENERGÉTICO Y MODELADO MATEMÁTICO DE LA DESCOMPOSICIÓN TÉRMICA DEL CUESCO Y DEL RACIMO DEL FRUTO VACÍO DE LA PALMA AFRICANA (*)

AUTORES: CARLOS JUNIOR ARIAS HERNANDEZ, JULIAN FERNANDO MANRIQUE PINTO (**)

PALABRAS CLAVES: Biomasa; Isoconversional; Termogravimetría; Pirolisis; Combustión.

DESCRIPCIÓN: El objetivo de esta investigación es estudiar el comportamiento de la pirólisis y las características de dos residuos colombianos de la palma africana (racimo de fruto vacío (EFB) y cuesco (PKS)) y los efectos de su mezcla mediante el análisis termogravimétrico (TGA). La mezcla estudiada se preparó con una relación de peso del 50%. Los experimentos TGA se implementaron en atmósfera inerte (argón, 99,99%), velocidad de flujo de 50 ml / min y con diámetro medio de partícula de 0,250 mm y cuatro velocidades de calentamiento diferentes de 1,25 °C/min, 2,5 °C/min, 5°C/min y 10°C/min en la rampa de temperatura de 25 °C a 900 °C. Para encontrar los parámetros cinéticos se aplicaron los métodos de iso-conversion de Friedman y Vyazovkin, los resultados obtenidos sugirieron que la cinética de la EFB, la PKS y la mezcla obedecen a una reacción más compleja, por lo tanto, fue propuesto un modelado por un mecanismo tres reacciones paralelas (IPRS). Finalmente, los resultados obtenidos por el mecanismo de tres reacciones paralelas fueron más precisos, describiendo con un ajuste inferior al 4% por el criterio de desviación media el proceso de descomposición térmica y de las propiedades físico-químicas se concluyó que la PKS es un recurso potencial de la energía térmica y las propiedades del EFB se mejoran significativamente con la mezcla.

(*) Trabajo de grado

(**) Facultad de Ingenierías Físico-Mecánicas. Escuela de ingeniería Mecánica. Director: Ing. Yesid Javier Rueda Ordóñez

ABSTRACT

TITLE: ANALYSIS OF ENERGETIC POTENTIAL AND MATHEMATICAL MODELING OF THE THERMAL DECOMPOSITION OF THE PALM KERNEL SHELL AND EMPTY FRUIT BRUNCH OF THE AFRICAN OIL PALM. (*)

AUTHORS: CARLOS JUNIOR ARIAS HERNANDEZ, JULIAN FERNANDO MANRIQUE PINTO (**)

KEYWORDS: Biomass; Iso-conversion; IPRS; Thermogravimetry; Pyrolysis; Combustion; Palm Kernel shell; Palm empty fruit bunch.

DESCRIPTION: This research aims to investigate the pyrolysis behavior and characteristic of two African oil palm wastes from Colombia (empty fruit brunch (EFB) and palm kernel shell (PKS)) and the effects of its blend by means of the thermogravimetric analysis (TGA). The studied blend sample was prepared at the 50% weight ratio. The TGA experiments were implemented in inert atmosphere (Argon, 99.99%), flow rate of 50 mL/min and particle mean diameter of 0.250 mm and four different heating rates of 1.25 °C/min, 2.5 °C/min, 5 °C/min and 10 °C/min in the ramp of temperature from 25 °C to 900 °C. In order to find the kinetic triplet out the iso-conversion methods of Friedman and Vyazovkin were applied but the results obtained suggested that the kinetic of the EFB, the PKS and the blend obeys a complex reaction pathway, thus, a modelling by a mechanism of three-parallel reactions (IPRS) was proposed. Finally, the results obtained by the mechanism of three parallel reactions were more accurate, describing with a fit lower than 4% by average deviation criteria the thermal decomposition process and from the physical-chemical properties it was concluded that the PKS is a potential resource of thermal energy and the properties of the EFB can be significantly enhanced with the blend.

(*) Bachelor Thesis

(**) Facultad de Ingenierías Físico-Mecánicas. Escuela de ingeniería Mecánica. Director: Ing. Yesid Javier Rueda Ordóñez

Introduction

Currently, biomass is becoming an important investigation issue as an alternative energetic source through several processes, such as combustion, gasification, liquefaction and pyrolysis, since the environmental impact of the current methods for obtaining energy based on fossil fuels has become a critical environmental affair. Developing countries have a farming-based economy, therefore, research focused on biomass potential gives an important opportunity of growth on a country such as Colombia which is the fourth producer of African oil palm in the world and first producer in Latin America.

Nowadays, there are 5000 producers of African oil palm and they are distributed in 124 municipalities of 20 departments, generating more than 140000 direct and indirect employments to the Colombian's families. In 2017, 452435 ha were required for a production of approximately 1632667 tons in the processing of African oil palm (Eleais guineensis).

There are a lot of products that derivate from the African oil palm, as cooking oil, cosmetic, oil paint, soap, candle, detergent, ink, and biofuel. In the processing of African oil palm are generated tons of residues which are mainly composed by empty fruit bunch (EFB), fiber and kernel shells (PKS). Due its characteristics, the empty fruit bunch is used as fertilizer in the agroindustry and the kernel shells are commonly used as solid fuels for boilers, i.e., in direct combustion process. Therefore, it is a priority to investigate the thermal behavior of this biomass, since it will contribute in the development of new technologies for the regional agroindustry for a better disposal of this wastes.

This work aims to analyze the physical-chemical characteristics and to understand the thermal decomposition process of the palm kernel shell, empty fruit bunch, and the blend between them through thermogravimetric analysis in argon atmosphere. Also, to obtain the kinetic triplet by through model-free methods and master plots for one global reaction mechanism, and as an alternative, a kinetic reaction mechanism based on independent parallel reactions is proposed. This study is structured in two chapters; the first is focused in the palm kernel shell behavior, and the purpose of the second chapter, is to study the empty fruit brunch and analyze its properties as it is blended with the kernel shell.

1 Objectives

1.1 General objective

To evaluate the energetic potential from the palm kernel shell and the empty fruit brunch of the African oil palm for studying its viability as energetic source.

1.2 Specific objectives

- Characterize the physical-chemical properties of the biomasses and a blend level of 50% of mass proportion between them.
- Characterize the thermal decomposition of the biomass and its blend by thermogravimetric analysis.
- Determinate the heating value of the biomasses and its respective blend.
- Obtain the mathematical model of the kinetics of the thermal decomposition from the biomass and its blend.

2 Kinetic analysis of the thermal decomposition of the kernel shell from the oil palm harvested in South America

2.1 Introduction

Currently, biomass is considered as one of the most promising alternatives to fossil fuels, and present interesting characteristics as a raw material for obtaining renewable energy through the several processes, such as combustion, gasification, liquefaction, and pyrolysis (Knežević, 2009). Nowadays, Colombia is going through a stage of post-conflict, in which people from the countryside will return to their lands. For this reason, there is a potential for growth in farming such as the African oil palm crops.

In 2017, 452 435 ha were required for a production of approximately 1 632 667 ton (Fedepalma, 2018). In the processing of African oil palm (*Eleais guineensis*) are generated a higher amount of residues, which are mainly composed of empty fruit bunch, fiber and kernel shells. Nowadays, kernel shells are commonly used as solid fuels for boilers, i.e., in the combustion process (Van Dam, J., 2016). Therefore, it is a priority to investigate the thermal behavior of this biomass, since it will contribute to the development of new technologies for the regional agroindustry.

The major components of the lignocellulosic biomass can be classified as cellulose, hemicellulose, and lignin (Rueda-Ordóñez & Tannous, 2018; Xiang et al., 2018). The cellulose is one of the cell wall structure components of vegetal cells, this linear polymer composition is in the order of 2000 and 14000 β-glucose units (Carreño et al., 2012). The hemicellulose is composed by different branched polysaccharides such as xylose, mannose, glucose, galactose, and it is located between the cellulose and the lignin, working as a link between them (Oliva, J., 2003; Yang et al.,

2007; Dhyani & Bhaskar,2018). The lignin has a complex structure and is considered amorphous, formed by aromatic groups of phenolic nature, and its function is to keep the fibers together, protecting them from microbial attacks and ensure the cell wall impermeability (Barroso, 2010; Dhyani & Bhaskar,2018).

The biomass thermal decomposition process can be divided into four main stages: moisture release, cellulose, hemicellulose, and lignin decomposition, respectively. The cellulose, hemicellulose, and lignin main weight loss occur at the temperature ranges of 220-315 °C, 315-400 °C, and 100-900 °C, respectively. The biomass thermal decomposition can be considered as the superposition of the reactions of each biomass major components (Yang et al., 2007; Liu et al., 2011; Cai et al., 2013).

The research of the kinetics of thermal decomposition of solid fuels, as well as biomass, is normally carried out through the technique of thermogravimetry since this process is governed by solid-state reactions. Also, allowing to study the temperatures that generate partial thermal decomposition, and analyzing the change of mass by the effects of temperature variation in controlled conditions (Wróblewski & Ceran, 2016).

The kinetic analysis of biomass thermal decomposition is commonly studied by applying three different solid-state reaction mechanisms, such as one global reaction, consecutive reactions, and parallel reactions (Rueda-Ordóñez & Tannous, 2018). The iso-conversion methods, which are used in the analysis of one global reaction has been under development since 1951 (Van Krevelen et. al,1951), in which, through the years many alternative solutions have been proposed by several authors such as Friedman (1964) (FD), Ozawa (1965), Flynn & Wall (1966) (OFW), Braun, Burnham & Reynolds (1991) (KAS) and Vyazovkin (2000) (VZ).

In solid-state reaction kinetics, is fundamental to obtain the triplet of parameters (activation energy, (*Ea*) reaction order (*n*), and pre-exponential factor (*A*)) which constitute chemical reaction models, since, with only one parameter, e.g., activation energy, it is impossible to describe the overall process. Then, in order to complete the kinetic parameters, the chemical reaction models for a global reaction is normally determined by means of the Master Plot methodology that emerged from the same definition of the iso-conversion integral methods and consists in a comparison between the results obtained by experimental data and the theoretical chemical reaction models. This methodology is commonly implemented as showed in several works (Vyazovkin et al., 2011; Mishra and Bhaskar, 2014; Rueda Ordóñez & Tannous, 2015; Chen et al., 2017; Wadhwani et al., 2017). These chemical reaction models are the first and nth order (F1), one-dimensional diffusion (D1), Two-dimensional diffusion (D2), Three-dimensional diffusion (D3), and Three-dimensional diffusion Ginstling-Brounshtein (D4).

The definition of the chemical reaction model is an important step in the kinetic study, and consequently, if it is erroneously proposed, the kinetic parameters will have no sense. Therefore, the Master Plot methodology presents the correct way to determinate the reaction model (Vyazovkin et al., 2011).

The independent parallel reactions scheme is one of the most widely used reaction mechanisms to describe the kinetics of thermal decomposition of lignocellulosic material (Santos et al., 2010). In this mechanism, the reactions are related to the main components of the biomass, and these are known as pseudo-components. The main pseudo-components in a lignocellulosic material are hemicellulose, cellulose, and lignin. (Rueda-Ordóñez et al., 2015).

Table 1 presents the activation energy determined by different authors for several biomasses applying iso-conversion methods. Da Silva et al. (2018) studied waste wood from reforestation:

Eucalyptus benthamii, *Eucalyptus dunni*, and *Pinus elliotti*. The results obtained with FD presented a higher activation energy compared with the other methods, however, VZ showed that the decomposition process of *Eucalyptus benthamii* and *Eucalyptus dunni* occurs as a multi-step process. On the other hand, for *Pinus elliotti*, a satisfactory fit to the experimental data was obtained. Mishra & Mohanty (2018), determined the kinetic parameters of three waste biomass: Areca nut husk, Pine Sawdust, and Sal Sawdust. The authors studied the conversion level from zero to 0.7 and the activation energy obtained with FD was slightly higher than KAS and OFW but for Pine Sawdust FD was slightly lower than the others. Kongkaew et al. (2015), obtained the kinetic parameters for the rice straw by KAS and OFW describing the complexity of the pyrolysis process. Lee et al. (2017), presented the kinetic parameters for the PKS and the empty fruit brunch. The kinetic study was carried out from the conversion level 0.2 to 0.7. Rueda-Ordoñez & Tannous (2015) studied the sugarcane straw, the activation energies obtained varied from 154.1 kJ/mol to 177.8 kJ/mol.

Table 2 presents the activation energy determined by different authors for several biomasses applying the three-independent parallel reactions mechanism, in which, each reaction corresponds to the hemicellulose (reaction 1), cellulose (reaction 2) and lignin reaction (reaction 3) respectively, it is important to remark that the no previous studies were available in the literature of modelling for the studied biomass by using this mechanism. Yu et al. (2015) implemented a three-independent parallel reaction mechanism to understand the kinetic behavior of bamboo on a pyrolysis process, obtaining the kinetic triplet for each lignocellulosic pseudo-component reaction. The authors also analyzed samples that had a fungal pretreatment, in order to study its effect on the thermal decomposition, by comparing the differences in the kinetic behavior. Sfakiotakis & Vamvuka (2015), studied the kinetics of different biomass wastes by using a modified IPRS, in

which the activation energy was kept constant for each heating rate, altering only the value of the pre-exponential factor, improving the accuracy in the obtained model.

Table 1.
The activation energy for several biomasses determined through iso-conversion methods.

Author	Material	Ea (kJ/mol)
Da Silva et al. (2018)	Eucalyptus Benthamii	142.98[a] 133.31[b]
	Eucalyptus Dunii	147.71[a] 137.98[b]
	Slash pine	155.46[a] 145.70[b]
Mishra and Mohanty (2018)	Areca nut husk	184.61[a] 179.47[c] 171.24[d]
	Pine Sawdust	168.58[a] 179.29[c] 171.66[d]
	Sal Sawdust	181.53[a] 156.58[c] 148.88[d]
Kongkaew et al. (2015)	Rice Straw	192.66[c] 193.60[d]
Lee et al. (2017)	EFB	169.76[c] 169.36[d]
	PKS	205.34[c] 205.70[d]
Rueda-Ordoñez & Tannous (2015)	Sugar cane Straw	154.0[a]

[a]FD; [b]VZ; [c]OFW; [d]KAS

This study aims to investigate the thermal decomposition process of palm kernel shell (*PKS*) in argon atmosphere through thermogravimetric analysis. Also, iso-conversion and Master Plots methods were used to determinate the kinetic triplet of parameters. Besides, a kinetic mechanism based on independent parallel reactions was also proposed.

Table 2.
Kinetic parameters for thermal decomposition of biomass in IPRS.

Author	Material	Reaction 1		Reaction 2		Reaction 3	
		Ea (kJ/mol)	log A (log 1/s)	Ea (kJ/mol)	log A (log 1/s)	Ea (kJ/mol)	log A (log 1/s)
Sfakiotakis & Vamvuka (2015)	Olive pruning	94.5	8.16	168.3	13.51	41.1	0.98
Yu et al. (2015)	Olive Kernel	87.5	7.97	132.1	13.11	44.1	2.65
	Vine Shoots	106.5	9.36	149.6	12.23	38.1	0.86
	Bamboo	167.32	13.00	241.78	17.99	74.54	4.03

2.2 Materials and methods

2.2.1 Biomass preparation and characterization. Palm kernel shell (*PKS*) from the African oil palm (Eleais guineensis) was the biomass selected for analysis in this work. The biomass was ground and sieved to a mean particle size of 250 μm for the thermogravimetric experiments.

The PKS samples were obtained from the surroundings of Puerto Wilches, Colombia, and is located in the northeastern region of the country at the coordinates 7° 20′ 54″ N, 73° 53′ 54″ W with an average altitude of 75 meters above the sea level. According to (Peel, Finlayson ‘'and McMahon, 2007) Puerto Wilches is located in a tropical rainforest weather zone.

The moisture content (*M*), ash content (*Ash*), and volatile content (*VM*) were obtained following the standards ASTM E871-82, ASTM E1755-01, and ASTM E872-82, respectively, and the fixed carbon (*FC*) was calculated by difference on dry basis. Elemental analysis was carried out by using the Eqs. (1), (2), and (3), in which C, H, and O are the percent of carbon, hydrogen, and oxygen, respectively. (Parikh et al., 2007)

$$C=0.637FC+0.455VM \quad (1)$$

$$H=0.052FC+0.062VM \quad (2)$$

$$O=0.304FC+0.476VM \quad (3)$$

In order to determine the higher heating value (HHV), was used an oxygen calorimetric bomb IKA C200 and applied the standard ASTM D240-09. The lower heating value (LHV) was calculated using Eq. (4) as follows (Monir et al., 2018).

$$LHV = HHV - 2.260\left(\frac{9H}{100}+\frac{M}{100}\right) \quad (4)$$

2.2.2 Thermal Decomposition Analysis. The thermal analysis was carried out using a thermogravimetric analyzer NETZSCH STA 449F3. The sample weight loss was measured from the room temperature up to 1000°C using four different heating rates of 1.25 °C/min, 2.5 °C/min, 5 °C/min and 10 °C/min. In order to obtain reliable and accurate results, prior to the experiments, the samples were dried, and the thermogravimetric analyzer was evacuated with a vacuum pump (exclusion of oxygen traces). The initial mass in each experiment was around 7 mg with argon as an inert atmosphere, using a flow rate of 50 mL/min. The sample weight loss was measured in steps of 5 seconds or 12 samples/min**.**

2.2.3 Thermal Decomposition and Kinetic Modeling. In order to make a quantitative comparison of the thermal decomposition curves at different heating rates, the thermogravimetry data (*TGA*) and their derivatives (*DTG*) were normalized using Eqs. (5) and (6), respectively, in which m_i is the initial mass, m is the mass at time t, and w is the normalized mass. In Eq. (6) dm/dt represents the experimental DTG in mg/s, and dw/dt is the normalized DTG.

$$\boldsymbol{w = \frac{m}{m_i}} \tag{5}$$

$$\boldsymbol{\frac{dw}{dt} = \frac{dm}{dt}\frac{1}{m_i}} \tag{6}$$

2.2.4 Thermal decomposition kinetics. The PKS thermal decomposition kinetics was determined in two steps: (i) application of iso-conversion method, (ii) application of a mechanism of three independent parallel reactions. In the first step, were applied the iso-conversion methods in order to obtain a first approach of the activation energy variation with the conversion. In the second step, were assumed three independent parallel reactions, and the activation energies determined in the previous step were used as a first approach in the iterative process.

The determination of the experimental conversion (α_e) and experimental conversion rate $(d\alpha/dt)_e$ was carried out with Eqs. (7) and (8). Eq. (7) represents the biomass main conversion into gases and volatile released in the selected decomposition range, in which w_i, w, and w_f are the normalized mass at the beginning, at the time t and at the end of the decomposition range.

$$\boldsymbol{\alpha_e = \frac{w_i - w}{w_i - w_f}} \tag{7}$$

$$\boldsymbol{\left(\frac{d\alpha}{dt}\right)_e = -\frac{dw}{dt}\left(\frac{1}{w_i - w_f}\right)} \tag{8}$$

Eq. (9) is based on the Arrhenius's law, and represents the theoretical conversion rate (dα/dt)t, in which *Ea* is the activation energy (kJ/mol), *A* is the pre-exponential factor (s-1), *β* is the heating rate, *R* is the universal gas constant (8.314 kJ/mol K), *T* is the absolute temperature, and *f(α)* is the conversion function depending on the conversion (*α*), the reactive concentrations and reaction order and according to the reaction mechanism proposed in this work.

$$\boldsymbol{\left(\frac{d\alpha}{dt}\right)_t = A[f(\alpha)]\left[exp\left(\frac{-Ea}{R \cdot T}\right)\right]} \tag{9}$$

- ***Iso-conversion methods***. In this kinetic study, two iso-conversion methods: Vyazovkin integral method and Friedman differential method were applied. For the analysis, four heating rates; β_1=1.25 °C/min, β_2=2.5 °C/min, β_3=5.0 °C/min and β_4=10 °C/min were used. Besides, 19 conversion levels were defined from 0.05 to 0.95 with a step of 0.05.

➢ *Friedman method.* The differential method developed by Friedman, (1964) was the first developed. The model was derived from applying the natural logarithm in Eq. (9), providing the final form of the model, presented in Eq. (10).

$$\ln\left(\frac{d\alpha}{dt}\right) = \ln(A) + \ln[f(\alpha)] - \left(\frac{Ea}{R \cdot T}\right) \quad (10)$$

Thus, in order to find the activation energy, for each conversion level, it was plotted the curve *ln(dα/dt)* as a function of *1/T*, and the slope of the straight line formed was multiplied by *R*, providing the activation energy.

➢ *Vyazovkin method.* The integral methods solve the Eq. (9) by integration from Eq. (11), in which $g(\alpha)_t$ is the integrated form of the conversion function, $f(\alpha)$. Eq. (11) represents the proximate solution of Eq. (9) by integration, since no analytical solutions exist. Therefore, in the right side of Eq. (11) is presented the function *p(x)* which is solved by applying the 8th degree rational approximation developed by Pérez-Maqueda & Criado, (2000) and presented in Eq. (12), considering *x =Ea/(R·T)*.

$$g(\alpha)_t = \int \frac{1}{f(\alpha)}\, d\alpha = \frac{A \cdot Ea}{R \cdot \beta}\left\{-\left[\frac{\exp(x)}{x}\right] + \int_{-\infty}^{x}\left[\frac{\exp(x)}{x}\right] dx\right\} = \frac{A \cdot Ea}{R \cdot \beta}\, p(x) \quad (11)$$

$$p(x) = \left(\frac{exp(-x)}{x}\right) \cdot \left(\frac{x^7+70x^6+1886x^5 24920x^4+170136x^3+577584x^2+844560x+357120}{x^8+72x^7+2024x^6+28560x^5+216720x^4+880320x^3+1794240x^2+1572480x+403200}\right) \quad (12)$$

The nonlinear integral method Vyazovkin, (2000) is represented by Eq. (13), in which $I\left(E_\alpha, T_i(t_\alpha)\right)_\alpha = P(x) \cdot (E_\alpha/R)$ and the apparent activation energy value E_α for each conversion level can be determined by minimizing the function $\emptyset$.

$$\emptyset = \sum_{i}^{n} \sum_{j \neq i}^{n} \frac{\boldsymbol{I\left(E_\alpha, T_i(t_\alpha)\right) \cdot \beta_j}}{\boldsymbol{I\left(E_\alpha, T_j(t_\alpha)\right) \cdot \beta_i}} \quad (13)$$

In this work were used four heating rates $\beta_1 = 1.25\ ℃/min$, $\beta_2 = 2.5\ ℃/min$, $\beta_3 = 5\ ℃/min$ and $\beta_4 = 10\ ℃/min$ and therefore, Eq. (13) can be rearranged as Eq. (14).

$$\emptyset = \frac{I(E_\alpha,T(t_\alpha))_{\beta_1}\cdot\beta_2}{I(E_\alpha,T(t_\alpha))_{\beta_2}\cdot\beta_1} + \frac{I(E_\alpha,T(t_\alpha))_{\beta_1}\cdot\beta_3}{I(E_\alpha,T(t_\alpha))_{\beta_3}\cdot\beta_1} + \frac{I(E_\alpha,T(t_\alpha))_{\beta_1}\cdot\beta_4}{I(E_\alpha,T(t_\alpha))_{\beta_4}\cdot\beta_1} + \frac{I(E_\alpha,T(t_\alpha))_{\beta_2}\cdot\beta_1}{I(E_\alpha,T(t_\alpha))_{\beta_1}\cdot\beta_2} + \frac{I(E_\alpha,T(t_\alpha))_{\beta_2}\cdot\beta_3}{I(E_\alpha,T(t_\alpha))_{\beta_3}\cdot\beta_2} +$$

$$\frac{I(E_\alpha,T(t_\alpha))_{\beta_2}\cdot\beta_4}{I(E_\alpha,T(t_\alpha))_{\beta_4}\cdot\beta_2} + \frac{I(E_\alpha,T(t_\alpha))_{\beta_3}\cdot\beta_1}{I(E_\alpha,T(t_\alpha))_{\beta_1}\cdot\beta_3} + \frac{I(E_\alpha,T(t_\alpha))_{\beta_3}\cdot\beta_2}{I(E_\alpha,T(t_\alpha))_{\beta_2}\cdot\beta_3} + \frac{I(E_\alpha,T(t_\alpha))_{\beta_3}\cdot\beta_4}{I(E_\alpha,T(t_\alpha))_{\beta_4}\cdot\beta_3} + \frac{I(E_\alpha,T(t_\alpha))_{\beta_4}\cdot\beta_1}{I(E_\alpha,T(t_\alpha))_{\beta_1}\cdot\beta_4} +$$

$$\frac{I(E_\alpha,T(t_\alpha))_{\beta_4}\cdot\beta_2}{I(E_\alpha,T(t_\alpha))_{\beta_2}\cdot\beta_4} + \frac{I(E_\alpha,T(t_\alpha))_{\beta_4}\cdot\beta_3}{I(E_\alpha,T(t_\alpha))_{\beta_3}\cdot\beta_4} \quad (14)$$

➢ *Determination of the conversion function.* The evaluation of Eq. (11) in the conversion level of 50 %, allows obtaining Eq. (15), in which $x_{0.5} = Ea/(R \cdot T_{0.5})$ and $T_{0.5}$ is the temperature in that conversion level.

$$g(0.5) = \frac{A \cdot E_a}{\beta \cdot R} p(x_{0.5}) \quad (15)$$

In order to remove the influence of the pre-exponential factor in the Master Plot, Eq. (11) is divided by Eq. (15) obtaining Eq. (16), in which $g(x)/g(x_{0.5})$ represents the theoretical Master Plot and $p(x)/p(x_{0.5})$ represents the experimental Master Plot.

$$\frac{g(\alpha)}{g(0.5)} = \frac{\frac{A \cdot Ea}{\beta \cdot R} p(x)}{\frac{A \cdot Ea}{\beta \cdot R} p(x_{0.5})} = \frac{p(x)}{p(x_{0.5})} \quad (16)$$

➢ *Determination of pre-exponential factor*. The determination of pre-exponential factor was carried out plotting $ln[(d\alpha/dt)/f(\alpha)]$ as a function of $1/T$, and from this data was carried out a linear regression, in which, the intersection with the axis Y represent the pre-exponential factor natural logarithm and the slope of the linear regression multiplied by the universal gas constant is the activation energy (Rueda-Ordóñez & Tannous, 2015). Eq. (17) shows the linearization of Eq. (9).

$$\boldsymbol{ln\left[\frac{(d\alpha/dt)}{f(\alpha)}\right] = ln(A) - \frac{Ea}{R \cdot T}} \quad (17)$$

- ***Mechanism of independent parallel reactions*.** The chemical reaction model is represented by the Eq. (18), where F_i, the volatile mass fraction, is related with each pseudo-component and j is the total number of reactions.

$$\boldsymbol{\frac{d\alpha}{dt} = \sum_{i}^{j} F_i \frac{d\alpha_i}{dt} = \sum_{i}^{j} F_i A_i \exp\left(-\frac{E_i}{RT}\right) f(\alpha_i)} \quad (18)$$

In order to obtain the theoretical conversion for the solution of Eq. (9) and Eq. (18), the temperature was controlled by Eq. (19), in which T_0=150 °C, corresponding to the beginning of the thermal decomposition and the end of the drying stage. Also, β represent

the heating rate (°C/s), and t (s) the time, following Eq. (20), in which t_0 was the time at 150 °C and h the step selected (5 s).

$$T = T_0 + \beta \cdot t \tag{19}$$

$$t = t_0 + h \tag{20}$$

Finally, the solution of the theoretical conversion and determination of kinetic parameters in the independent parallel reactions mechanism were carried out applying the first order Euler method, and the obtained curve was fitted to the experimental data by the least squares method. The quality of fit was measured with the average deviation (*AD*) presented in Eq. (21), and was applied a reliability criterion of *AD* < 3%. In Eq. (21), $(d\alpha/dt)_{e,max}$ is the maximum experimental conversion rate, *e* and *t* are experimental and theoretical data, and *N* the number of experimental points considered were 9408, 4704, 2352 and 1176 for 1.25 °C/min, 2.5 °C/min, 5 °C/min, and 10 °C/min, respectively.

$$\boldsymbol{Error\ porcentage}(\%) = \left[\frac{\sqrt{\frac{\sum_{i=0}^{N}\left[(y)_{experimental} - (y)_{theoretical}\right]^2}{N}}}{(y)_{experimental,maximum}}\right]\mathbf{100} \tag{21}$$

When $\boldsymbol{y = \frac{d\alpha}{dt}}$, the error percentage will be denoted as AD.
When $\boldsymbol{y = \alpha}$, the error percentage will be called AVP.

2.3 Results and Discussion

2.3.1 Biomass Characterization. In Table 3 are presented the results related to the kernel shell physical-chemical characterization, and show the values obtained for the proximate and ultimate analyses, and the heating value, comparing them with literature (Lee et al., 2017; Sukiran et al., 2017; Asadullah et al., 2018).

Table 3.
Physical-chemical properties of the PKS sample.

Author	This work	Lee et al. (2017)	M.A. Sukiran et al. (2017)	Asadullah et al. (2018)
Proximate analysis, mass % (dry basis)				
M	6.28 ± 0.16	4.53 ± 0.60	11.00 - 13.00	12.00
Ash	3.74 ± 0.06	7.54 ± 0.86	1.40 - 4.80	3.00
VM	85.38 ± 1.57	63.01 ± 3.80	82.70 - 84.40	74.00
FC	10.89	24.91 ±2.89	10.80 - 14.50	23.00
Ultimate analysis, mass % (dry basis)				
C	45.78	50,31	57.91	45.10
H	5.86	-	12.60	5.10
O	43.95	43,18	49.99	49.20
Heating Value, MJ/kg				
HHV	20.22 ± 0.21	19.72	20.09	-
LHV	18.89	-	-	-

According to Table 3, the proximate analysis values are in the same magnitude to the obtained by Sukiran et al., (2017), except for the *VM* that is slightly higher, which is compensated by the low *FC*. On the other hand, the proximate analysis results of lee et al., (2017), and Assadullah et al., (2018), differs considerably on the *VM* value which is also reflected by the higher *FC*. The ultimate analysis results are comparable according to the

presented values of the literature, as well as the high heating value (*HHV*) that only presents a variation with the *HHV* given by Lee et al., (2017), which is explained by the high ashes values of that study, since according to Jenkins et al, (1998) the ashes value considerably affects the heating value, since 1% reduces about 0.2 MJ/kg.

2.3.2 Biomass thermal decomposition. The TG and DTG curves of the palm kernel shell in an inert atmosphere of argon at different heating rates are shown in Fig. 1 (a) and (b), respectively. The thermal decomposition process can be divided into three stages: moisture evaporation, devolatilization, and carbonization.

The first stage or moisture evaporation stage takes place from room temperature to 150 °C, but in this study, the samples were dried before each analysis, therefore is not possible to determinate the moisture percent with this TG. In the temperature range between 150 °C and 200 °C, the mass variation was lower than 3% and is associated with the evaporation of some extractive compounds in the biomass. For this work, the effect of this process was considered negligible.

The devolatilization stage is observed in the temperature range between 200°C and 400°C in Fig 1(a). For this study, the volatilized mass was evaluated in 59.8%, 59.6%, 60.9% and 59.9% for the heating rates 1.25 °C/min, 2.5 °C/min, 5.0 °C/min, and 10.0 °C/min, respectively.

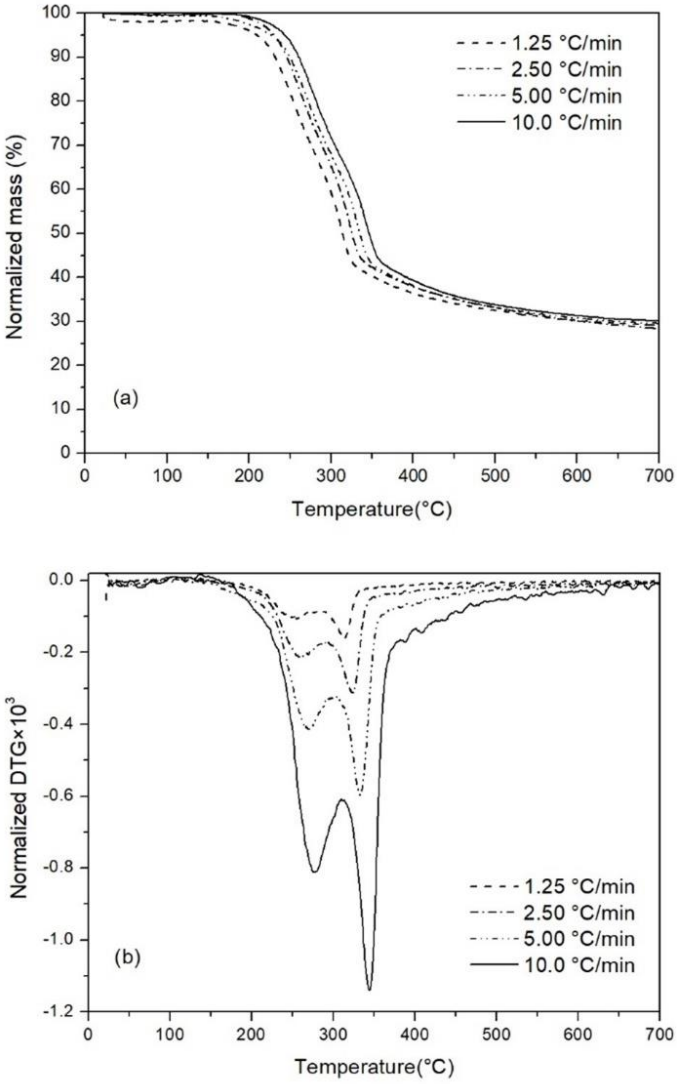

Figure 1. Palm kernel shell thermal decomposition (a) TG and (b) Normalized DTG as a function of temperature.

Finally, the final stage in the thermal decomposition process is the carbonization and take place after 400 °C. This stage is related mainly to the lignin decomposition. The mass variations in this stage were 7.27%, 9.54%, 8.56% and 9.92% at 700°C for the heating rates evaluated, respectively.

Regarding Fig 1(b), two major peaks are presented relating to hemicellulose, and cellulose decomposition, the first peak is related with the hemicellulose maximum decomposition rate at 252°C, 260°C, 270°C and 276°C for the heating rates evaluated, respectively. The second peak corresponds to the cellulose maximum decomposition rate at 314°C, 325°C, 333°C and 345°C for the related heating rates, respectively.

2.3.3 Kinetic modeling.

- ***Determination of the activation energy through iso-conversion analysis.*** In Fig. 2 are presented the apparent activation energy determined by the Friedman and Vyazovkin methods as a function of conversion. The activation energy obtained through Friedman method varied from 168.71 kJ/mol and a maximum of 191.50 kJ/mol, corresponding to 11.90% of variation between the minimum and maximum value of the average value that is 180.13 kJ/mol.

The apparent activation energy obtained by the method of Vyazovkin varied from 152.70 to 182.55 kJ/mol, and the behavior compared to the obtained through the method of Friedman follows a similar trend. This result shows that the global activation energy obtained by FD tends to be higher than the one from VZ, this result is also seen in the work of Da Silva et al. (2018), presented in Table 1. In addition, the change in the activation energy tends to be higher on each conversion level. This can be explained from the formulation of both methods, since the Friedman method is more sensitive to experimental error because of its differential nature, which is different from the Vyazovkin method that has an integrative formulation.

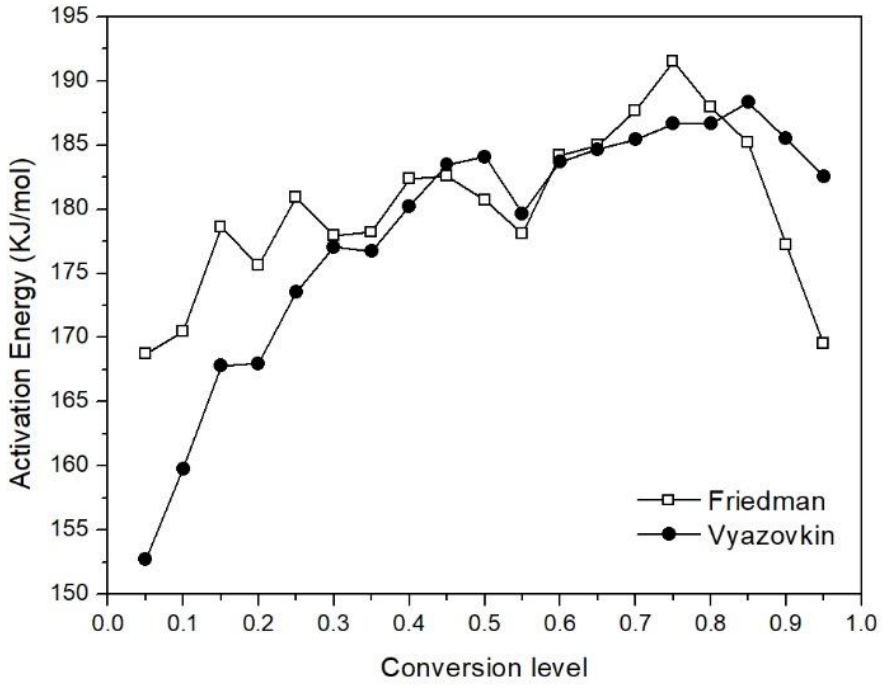

Figure 2. Apparent activation energy obtained by Friedman and Vyazovkin methods.

The results obtained by the isoconversional methods are 12.81% lower than the results presented by Lee et al. (2017) for the PKS, this difference could be attributed to the fact that the two samples presented a significant difference in the composition according to table 3 and to the different iso-conversion model, since the mathematical approach differs for each model. The results presented for the Pine Sawdust by Mishra & Mohanty (2018) are similar to the results obtained in the present study, showing just a difference of 3.03%, 0.16%, and 4.43% by the isoconversional methods FD, OFW and KAS, respectively.

- ***Reaction model and pre-exponential factor determination.*** Fig. 3 presents a comparison of the fitting of the chemical reaction models evaluated, which shows that none of the compared models can describe the behavior correctly. Table 4 shows that the closest was the D3 model equation with an AVP of 230.8%

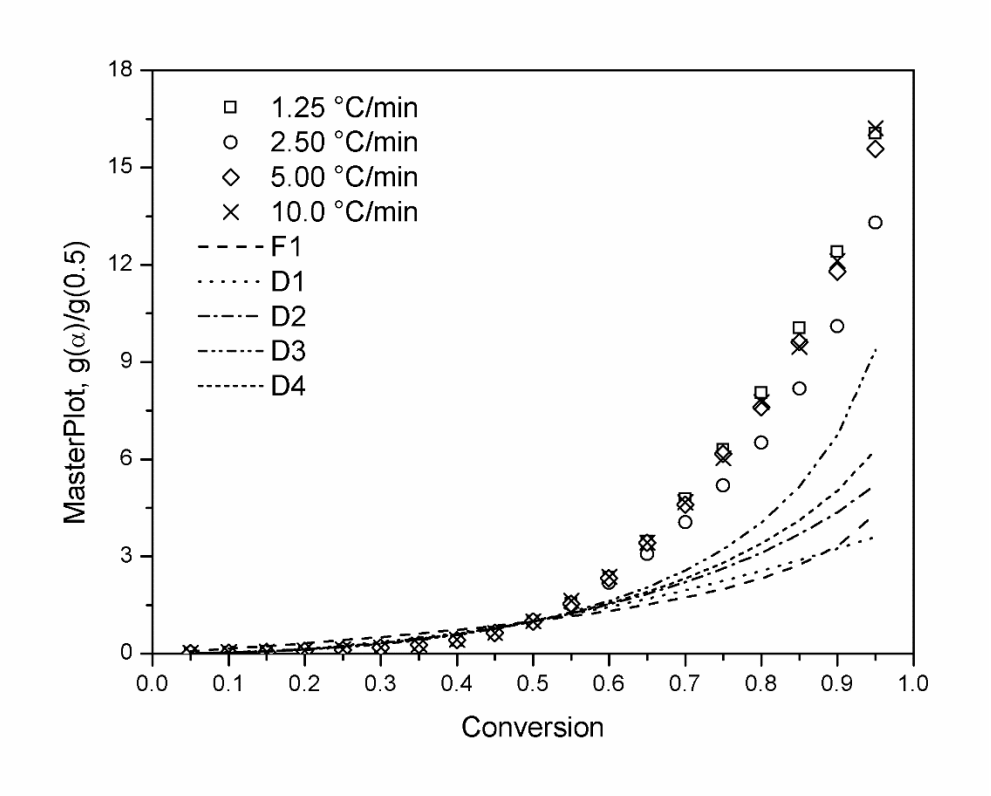

Figure 3. Comparison of the theoretical reaction models to the experimental results.

The resulting logarithm of the pre-exponential factor $Log_{10}(A)$ of 8,69 was obtained from the slope of the linearization of ln(dα/dt)/f(α) vs 1/T using the D3 reaction model presented in Fig. 3, and the obtained equation for this function was ln(dα/dt)/f(α)=-17.46(1/T)+21.84. As a forward step, the activation energy from the model was obtained by the multiplication of the slope by the universal gas constant (8.314 J/mol K).

Table 4.
Comparison between chemical reaction models and heating rates by AVP.

Symbol	$f(\alpha)$	AVP (%)
F1	$(1-\alpha)^n$	388.7
D1	$1/2\alpha$	394.6
D2	$\frac{1}{-ln(1-\alpha)}$	343.4
D3	$\left(\frac{1}{2}\right)\cdot\frac{3(1-\alpha)^{2/3}}{1-(1-\alpha)^{1/3}}$	230.8
D4	$\left(\frac{1}{2}\right)\cdot\frac{3}{(1-\alpha)^{-1/3}-1}$	312.4

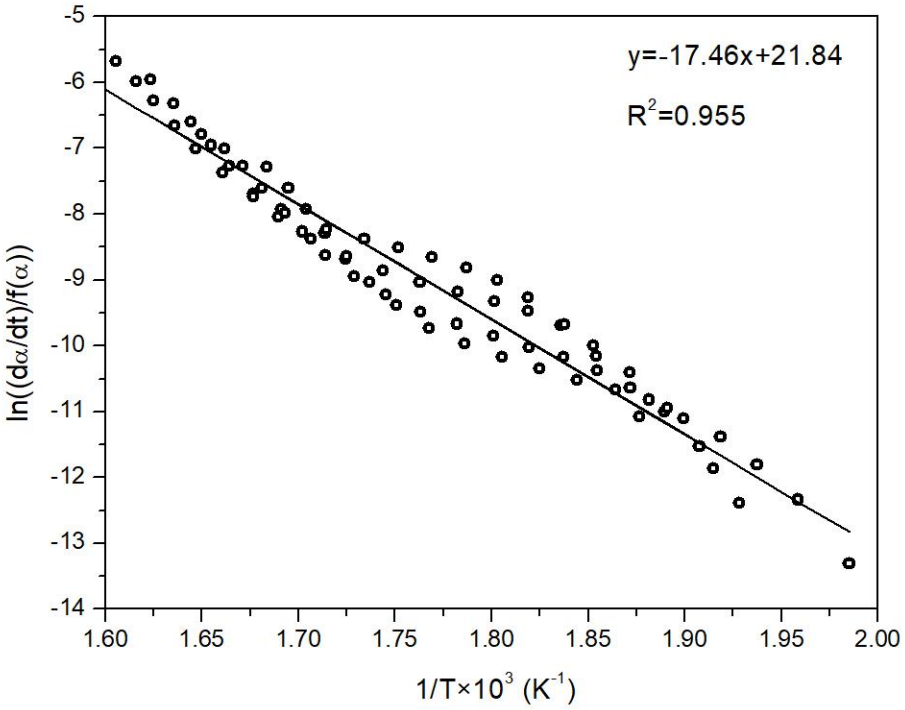

Figure 4. Linearization of ln(dα/dt)/f(α) as a function of 1/T

Table 5 presents the results obtained for activation energy, reaction model, and pre-exponential factor. The percentage error for all the heating rates was lower than 5%, and the activation energy used was 145.21 kJ/mol, determined from the linearization.

Table 5.
Iso-conversion Model kinetic parameters

Single global step model kinetic results					
f(α)		D3= $3/2*(1-\alpha)^{2}/3[1-(1-\alpha)^{1}/3]^{-1}$			
Ea	(kJ/mol)	145.21			
E_{aF}	(kJ/mol)	180.13			
E_{av}	(kJ/mol)	178.24			
$\log_{10}(A)$	($\text{Log}_{10}(S^{-1})$)	21.84			
Model validation					
B °C/min		1.25	2.5	5	10
Error (AVP) (%)		4.85	4.53	3.14	3.85

Ea: Activation energy
Eav: Apparent activation energy by Vyazovkin method
EaF: Apparent activation energy by Friedman method

Fig. 5 shows the normalized conversion α against temperature T, in which the solid lines were obtained with the kinetic parameters presented previously in Table 5. The comparison between theoretical and experimental data shows a great difference confirming that it does not represent correctly the behavior of the thermal decomposition.

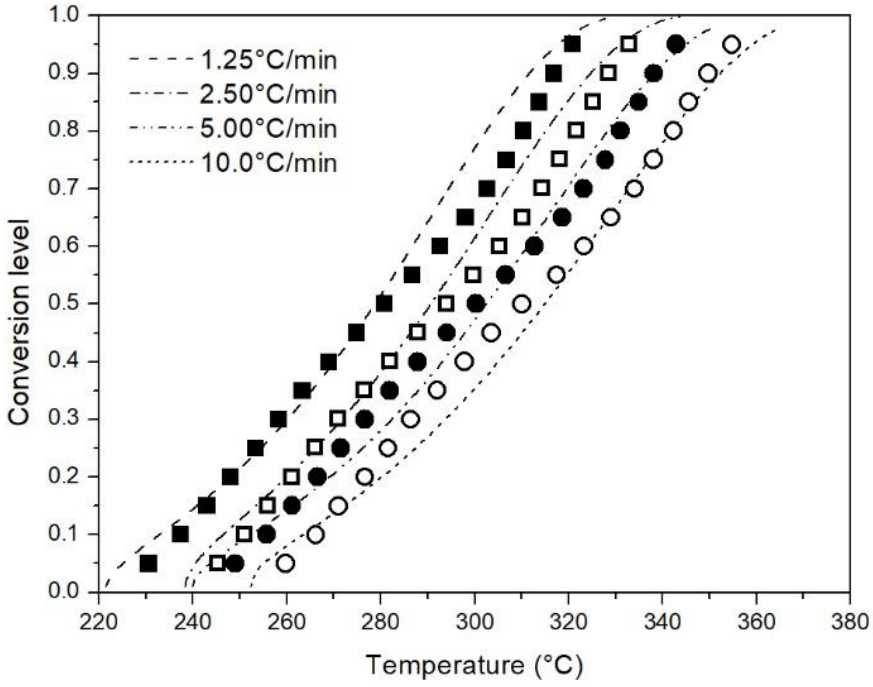

Figure 5. Conversion as a function of temperature. Theoretical (lines) and experimental at the heating rates of (■) 1.25°C/min, (□) 2.5°C/min, (●) 5 °C/min and (○) 10°C/min.

- ***Application of the independent parallel reaction scheme (IPRS).*** As the aforementioned analysis shows, the results obtained with iso-conversion methods do not provide an accurate modeling of the thermal behavior of the KS, and therefore, IPRS approach was considered.

Table 6 presents the kinetic triplet of the model assuming three-parallel reaction, in which each reaction was related to a lignocellulosic component. The activation energies related to the analyzed pseudo-component were 109.60 kJ/mol, 193.60 kJ/mol, and 34.67 kJ/mol, for hemicellulose (HC), cellulose (C) and lignin (L), respectively. The pre-exponential factor values were $\log_{10}A_{HC}$ =7.70, $\log_{10}A_{C}$ =14,13 and $\log_{10}A_{L}$ =-0,73. Also,

the fractions of the biomass composition (F) were 0,31 for HC, 0,33 for C, and 0,37 for L. Finally, the n^{th} reaction model was used for the three pseudo-components evaluated obtaining a first order for HC (Reaction 1, R1) and C (Reaction 2, R2) whereas, the lignin pseudo-component a reaction order of 1.75 was determined (Reaction 3, R3).

Table 6.
Results of the IPRS parameters for the PKS.

	Reaction kinetics		
	R1 (HC)	**R2 (C)**	**R3 (L)**
F(α)	$(1-\alpha)^n$	$(1-\alpha)^n$	$(1-\alpha)^n$
n	1	1	1,75±0.09
Ea (kJ) (kJ/Mol)	106.75± 0.96	186.25±3.50	31.33±0.29
Log10(A) ($Log_{10}(S^{-1})$)	7.71±0.02	13.86±0.24	-0.73±0.06
F	0.32±0.03	0.33±0.02	0.35±0.01

Ea: Activation energy

Table 2 presents the IPRS results of different analyzes made on samples from different biomasses. Nonetheless, for the biomass analyzed in this work, is scarse the literature in which the parallel reactions mechanism was applied to describe the thermal decomposition kinetics. Although, comparison with other biomass samples can be made, such as, the bamboo sample studied by Yu et al. (2015), which presents higher kinetic parameters to the ones obtained in the present work. Comparing with bamboo the PKS lignocellulosic pseudo-components require lower activation energy for thermal decomposition. This, is easily explained because both biomasses have a different composition, as the two of them

are from different species. Also, was verified that the values of the kinetic triplet from both biomass samples are in the interval described by (Rueda-Ordóñez et al., 2015).

The thermal decomposition was studied from 100 to 600 °C; since this interval occurs the pyrolysis reaction as stated by Rueda-Ordóñez et al. (2015). Table 7 presents the validation of the model through average deviation (AD) and (AVP) using criteria of 5% as accurate. Accomplishing less than 3% of error by average deviation (AD).

Table 7.
Results of the validation for the obtained model by IPRS for the PKS.

Model validation					
β (°C/min)	**1.25**	**2.5**	**5**	**10**	**Average**
AD (%)	2.97	2.89	2.88	2.98	2.93
AVP (%)	2.5	2.75	2.36	1.23	2.21

Fig. 5 describes the behavior obtained from each of the lignocellulosic components for the different heating rates analyzed. The reactions R1, R2, and R3 were related to each pseudo-component HC, C, L, respectively, and occurred in the intervals of 150-300 °C, 215-372°C and 100-900°C, respectively, following the expected behavior according to the temperatures ranges in literature (Yang et al., 2007; Liu et al., 2011; Cai et al., 2013). In addition, was observed that the cellulose and hemicellulose reactions tended to start with a temperature of about 50°C less than the expected, which was analyzed as an acceleratory behavior produced by the reaction model. Also, the dα/dt presented activity peaks at 265.65°C for hemicellulose, 314.20°C for cellulose and 361.98°C for lignin.

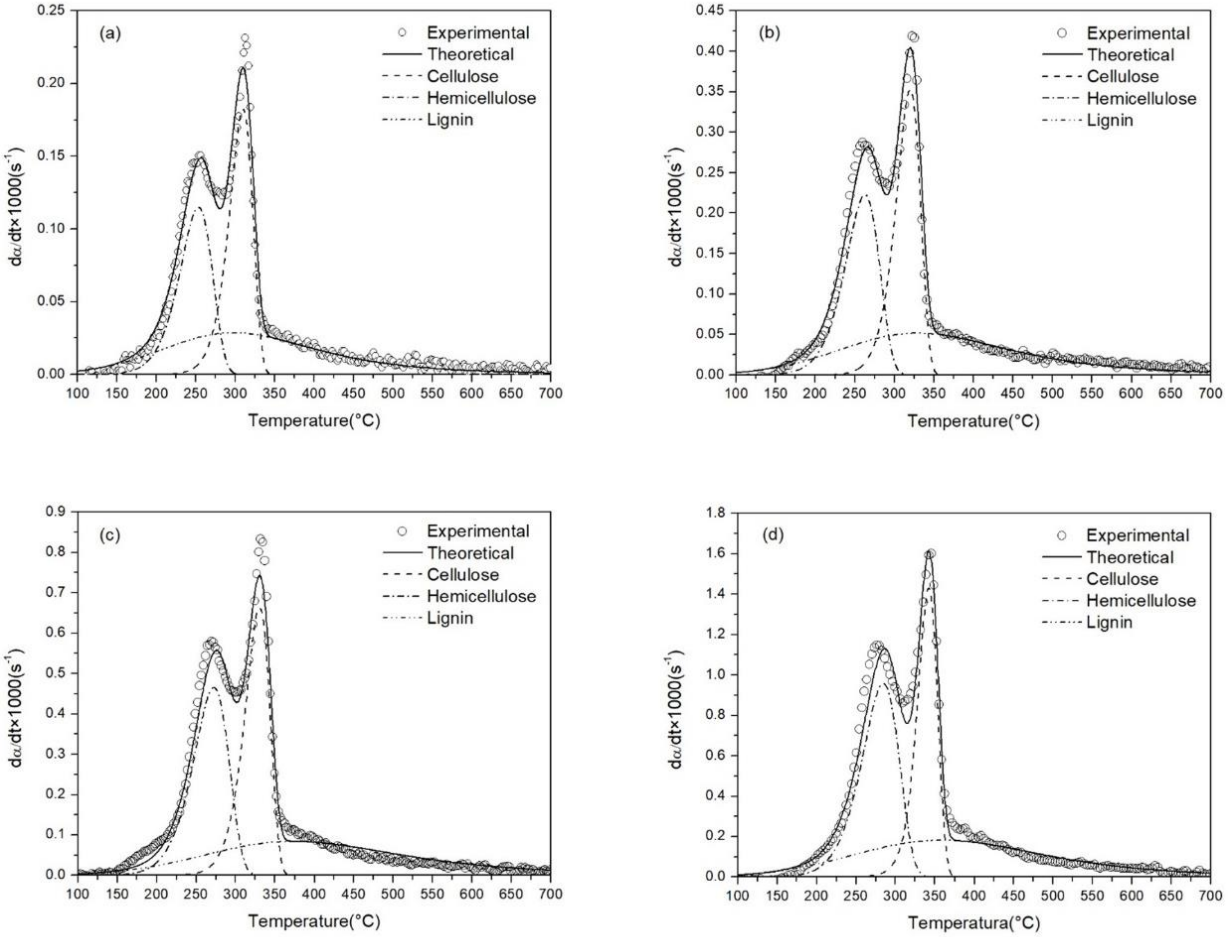

Figure 6. IPRS result of the PKS at the heating rates of (a) 1.25°C/min (b) 2.5 °C/min (c) 5.0 °C/min and (d) 10°C/min.

2.4 Conclusions

The palm kernel shell is presented as a good raw material for thermo-chemical processes due to its thermal characteristics and availability. Also, its thermal decomposition behavior was approximately described by iso-conversion methods, but it does not fit properly, meaning that the reliability of this reaction mechanism is low. Nevertheless, the modelling as a three-independent parallel reaction scheme described accurately the experimental data in the range of temperatures between 100 to 600 °C. Thus, the kinetic triplet determined for each independent reaction produced a modelling with an error less than 3% by average deviation criteria.

2.5 References

Asadullah, M., Rasid, N., Kadir, S., & Azdarpour, A. (2018). Production and detailed characterization of bio-oil from fast pyrolysis of palm kernel shell. *biomass and bioenergy, 59*(2013) 316-324. doi: 10.1016/j.biombioe.2013.08.037

Barroso Casillas, M., (2010). pretratamiento de biomasa celulósica para la obtención de etanol en el marco de una biorrefinería. (tesis de pregrado). Universidad Politécnica de Madrid. Recuperado de: http://oa.upm.es/10559/1/MIGUEL_BARROSO_CASILLAS.pdf

Braun, R. L., Burnham, A. K., Reynolds, J. G., & Clarkson, J. E. (1991). Pyrolysis kinetics for lacustrine and marine source rocks by programmed micropyrolysis. *Energy and Fuels*, *5*(1), 192–204. doi:10.1021/ef00025a033

Cai, J., Wu, W., Liu, R., & Huber, G. (2013). A distributed activation energy model for the pyrolysis of lignocellulosic biomass. *Green Chemistry, 15*(5), p.1331-1340. doi: 10.1039/C3GC36958G

Carreño Pineda, L., Caicedo Mesa, L., & Martínez Riascos, C., (2012). Técnicas de fermetación y aplicaciones de la celulosa bacteriana: una revisión. *Ingeniería y ciencia*, *8*(16), 307-335. Retrieved from: http://www.scielo.org.co/pdf/ince/v8n16/v8n16a12.pdf

Chan,Y.H., Quitain, A.,Yuzuo, S., Uemura, Y., Sasaki, M., & Kida, T. (2017) Liquefaction of palm kernel shell in sub- and supercritical water for bio-oil production, *Journal of the Energy Institute*, in press. doi:10.1016/j.joei.2017.05.009

Chen, R., Lu, S., Zhang, Y., & Lo, S. (2017). Pyrolysis study of waste cable hose with

thermogravimetry/Fourier transform infrared/mass spectrometry analysis. *Energy Conversion and Management, 153*, 83-92. doi:10.1016/j.enconman.2017.09.071

da Silva, J., Alves, J., Galdino, W., Andersen, S., & de Sena, R. (2018). Pyrolysis kinetic evaluation by single-step for waste wood from reforestation. *Waste Management, 72*, 265-273. doi:10.1016/j.wasman.2017.11.034

Dhyani, V., & Bhaskar, T. (2018). A comprehensive review on the pyrolysis of lignocellulosic biomass. *Renewable Energy, 129*, 695-716. doi:10.1016/j.renene.2017.04.035

Faizal, H., Shamsuddin, H., Heiree, M., Hanaffi, M., Rahman, M.R., Rahman, M., & Latiff, Z. (2018). Torrefaction of densified mesocarp fibre and palm kernel shell. *Renewable Energy, 122*, 419-428. doi:10.1016/j.renene.2018.01.118

Fedepalma. (2018). Con récord en producción de aceite de palma, sector palmero colombiano cierra 2017 con balance positivo. Retrieved from http://web.fedepalma.org/con-record-en-produccion-de-aceite-de-palma-sector-palmero-colombiano-cierra-2017-con-balance-positivo

Flynn, J. H., & Wall, L. A. (1966). General Treatment of the Thermogravimetry of Polymers. Journal of Research of the National Bureau of Standards, *70*(6), 487–523. doi:10.6028/jres.070A.044

Friedman, H. L. (1964). Kinetics of thermal degradation of char-forming plastics from thermogravimetry. *Application to a phenolic plastic. Journal of Polymer Science Part C: Polymer Symposia, 6*(1), 183–195. doi:10.1002/polc.5070060121

Jenkins, B., Baxter, L., Miles, T., & Miles, T. (1998). Combustion properties of biomass. *Fuel*

Processing Technology, *54*(1-3), 17-46. doi: 10.1016/s0378-3820(97)00059-3

Knežević, D. (2009). Hydrothermal conversion of biomass. (tesis de doctorado) University of Twente, Paises Bajos, p.11.

Kongkaew, N., Pruksakit, W., & Patumsawad, S. (2015). Thermogravimetric Kinetic Analysis of the Pyrolysis of Rice Straw. Energy Procedia, *79*, 663-670. doi: 10.1016/j.egypro.2015.11.552

Lee, X., Lee, L., Gan, S., Thangalazhy-Gopakumar, S., & Ng, H. (2017). Biochar potential evaluation of palm oil wastes through slow pyrolysis: Thermochemical characterization and pyrolytic kinetic studies. *Bioresource Technology*, *236*, 155-163. doi: 10.1016/j.biortech.2017.03.105

Liu, Q., Zhong, Z., Wang, S., & Luo, Z. (2011). Interactions of biomass components during pyrolysis: A TG-FTIR study. *Journal of Analytical and Applied Pyrolysis*, *90*(2), 213-218. doi: 10.1016/j.jaap.2010.12.009

Mishra, G., & Bhaskar, T. (2014). Non isothermal model free kinetics for pyrolysis of rice straw. *Bioresource Technology*, *169*, 614-621. doi:10.1016/j.biortech.2014.07.045

Mishra, R., & Mohanty, K. (2018). Pyrolysis kinetics and thermal behavior of waste sawdust biomass using thermogravimetric analysis. *Bioresource Technology*, *251*, 63-74. doi:10.1016/j.biortech.2017.12.029

Monir, M., Aziz, A., Kristanti, R., & Yousuf, A. (2018). Co-gasification of empty fruit bunch in a downdraft reactor: A pilot scale approach. *Bioresource Technology Reports*, *1*, 39-49. doi: 10.1016/j.biteb.2018.02.001

Monir, M., Aziz, A., Kristanti, R., & Yousuf, A. (2018). Co-gasification of empty fruit bunch in a downdraft reactor: A pilot scale approach. *Bioresource Technology Reports, 1,* 39-49. doi:10.1016/j.biteb.2018.02.001

Oliva Domínguez, J., (2003). *Efectos de los productos de degradación originados en la explosión por vapor de biomasa de chopo sobre Kluyveromyces marxianus*. (tesis doctoral). Universidad Complutense de Madrid. Recuperado de: http://biblioteca.ucm.es/tesis/bio/ucm-t26833.pdf

Ozawa, T. (1965). A new method of analizing thermogravimetric data. *Bulletin of the chemical Society of Japan, 38*(11),1881–1886. doi:10.1246/bcsj.38.1881.

Parikh, J., Channiwala, S., & Ghosal, G. (2007). A correlation for calculating elemental composition from proximate analysis of biomass materials. *Fuel, 86*(12-13), 1710-1719. doi:10.1016/j.fuel.2006.12.029

Peel, M., Finlayson, B., & McMahon, T. (2007). Updated world map of the Köppen-Geiger climate classification. *Hydrology and Earth System Sciences Discussions, 4*(2), 439-473. doi:10.5194/hess-11-1633-2007

Pérez-Maqueda, L., & Criado, J. (2000). *Journal Of Thermal Analysis And Calorimetry*, *60*(3), 909-915. doi:10.1023/a:1010115926340

Rueda-Ordóñez, Y., & Tannous, K. (2015). Isoconversional kinetic study of the thermal decomposition of sugarcane straw for thermal conversion processes. *Bioresource Technology, 196,* 136-144. doi:10.1016/j.biortech.2015.07.062

Rueda-Ordóñez, Y., & Tannous, K. (2018). Drying and thermal decomposition kinetics of

sugarcane straw by nonisothermal thermogravimetric analysis. *Bioresource Technology*, *264*, 131-139. doi: 10.1016/j.biortech.2018.04.064

Rueda-Ordóñez, Y., Tannous, K., & Olivares-Gómez, E. (2015). An empirical model to obtain the kinetic parameters of lignocellulosic biomass pyrolysis in an independent parallel reactions scheme. *Fuel Processing Technology*, *140*, 222-230. doi: 10.1016/j.fuproc.2015.09.001

Rueda-Ordóñez, Y.J., Baroni, E.G., Tinoco-Navarro, L.K., & Tannous, K., 2015. Modeling the kinetics of lignocellulosic biomass pyrolysis. In: Tannous, K. (Ed.), Innovative Solutions in Fluid-Particle Systems and Renewable Energy Management. IGI Global, Hershey, 92–130. doi:10.4018/978-1-4666-8711-0.ch004.

Santos, K., Lobato, F., Lira, T., Murata, V., & Barrozo, M. (2010). Diferential evolution method applied to kinetic parameters estimation of bagasse pyrolysis. *Asociación Argentina De Mecánica Computacional*, 2535-2548.

Sfakiotakis, S., & Vamvuka, D. (2015). Development of a modified independent parallel reactions kinetic model and comparison with the distributed activation energy model for the pyrolysis of a wide variety of biomass fuels. *Bioresource Technology*, *197*, 434-442. doi: 10.1016/j.biortech.2015.08.130

Sukiran, M., Abnisa, F., Daud, W., Bakar, N., & Loh, S. (2017). A review of torrefaction of oil palm solid wastes for biofuel production. *Energy Conversion And Management*, *149*, 101-120. doi: 10.1016/j.enconman.2017.07.011

Van Dam, J. (2016). Subproductos de la palma de aceite como materias primas de biomasa. *Palmas*, *37*(Especial Tomo II), 149-156.

Van Krevelen, D., Van Heerden, C., & Huntjens, F. (1951). Physicochemical aspects of the pyrolysis of coal and related organic compounds. *Fuel*, *30*, 253–259

Vyazovkin, S. (2000). Modification of the integral isoconversional method to account for variation in the activation energy. *Journal of Computational Chemistry*, *22*(2), 178-183. doi:10.1002/1096-987x(20010130)22:2<178::aid-jcc5>3.0.co;2-#

Vyazovkin, S., Burnham, A., Criado, J., Pérez-Maqueda, L., Popescu, C., & Sbirrazzuoli, N. (2011). ICTAC Kinetics Committee recommendations for performing kinetic computations on thermal analysis data. *Thermochimica Acta*, *520*(1-2), 1-19. doi: 10.1016/j.tca.2011.03.034

Wadhwani, R., Sutherland, D., Moinuddin, K. & Joseph, P. (2017). Kinetics of pyrolysis of litter materials from pine and eucalyptus forests. *Journal of Thermal Analysis and Calorimetry, 130*(3), 2035-2046. doi.org/10.1007/s10973-017-6512-0

Wróblewski, R., & Ceran, B. (2016). Thermogravimetric analysis in the study of solid fuels. *E3S Web Of Conferences*, *10*(00109). doi: 10.1051/e3sconf/20161000109

Xiang, Z., Liang, J., Morgan Jr., H.M., Liu, Y., Mao, H., & Bu, Q., 2018. Thermal behavior and kinetic study for co-pyrolysis of lignocellulosic biomass with polyethylene over Cobalt modified ZSM-5 catalyst by thermogravimetric analysis. *Bioresource. Technology*. *247,* 804-811. doi: 10.1016/j.biortech.2017.09.178

Yu, H., Liu, F., Ke, M., & Zhang, X. (2015). Thermogravimetric analysis and kinetic study of bamboo waste treated by Echinodontium taxodii using a modified three-parallel-reactions model. *Bioresource Technology, 185*, 324-330. doi: 10.1016/j.biortech.2015.03.005

3 Comparative Study of the Thermal Decomposition Kinetics and Characterization of the Empty Fruit Bunch from the Oil Palm with Blends of Palm Kernel Shell

3.1 Introduction

Nowadays, biomass is becoming an important research issue as an alternative energetic source, since the environmental impact of the current methods for obtaining energy based on the fossil fuels, which has become a critical environmental affair. Developing countries has a farming-based economy, therefore, research concentrated on biomass potential gives an important opportunity of growth on a country such as Colombia which is the fourth producer of African oil palm in the world and first producer in Latin America. In Colombia, there are 5000 producers of African oil palm (*Eleais guineensis*) and they are distributed in 124 municipalities, generating more than 140000 direct and indirect employments to the Colombian's families.

There are lot of products that derivate from the African oil palm, as cooking oil, cosmetic, oil paint, soap, candle, detergent, ink, and biofuel. In the processing of African oil palm are generated tons of residues which are mainly composed by empty fruit bunch (EFB), fiber, and kernel shells (PKS). Currently, per each ton of oil that is produced, 1.1 tons of empty fruit bunch are produced. Due its characteristics, the empty fruit bunch is used as fertilizer in the agroindustry.

The pyrolysis of lignocellulosic biomass is a thermochemical process that occurs in absence of an oxidizing agent, and involves several reactions occurring simultaneously, e.g. dehydration, depolymerization, fragmentation, rearrangement, repolymerization, condensation and carbonization (Quan et al., 2016). Therefore, predicting exact reaction mechanism is not possible (Mishra & Mohanty, 2018). The pyrolysis has some advantages compared with the combustion and gasification: lower temperature requirement, oxygen absent condition and production of

higher-quality oil (Chen et al., 2015). Also, this process allows transforming biomass into value added products, e.g. bio-char, bio-oil, fuels, synthesis gas, and chemicals (Rueda-Ordóñez et al., 2015).

Kinetic modeling of pyrolysis is a practical tool to describe the conversion processes and optimize the design of efficient reactors (Chen et al., 2015). By means of a thermogravimetric analyzer (TGA) and mathematical kinetic approaches, it is possible to determining the kinetic parameters: activation energy (*Ea*), pre-exponential factor (*A*) and reaction order (*n*). In this paper were applied two free models (Iso-conversion methods) to evaluate the kinetic parameters: Friedman (1964) (FD) and Vyazovkin (2000) (VZ). The Master Plot methodology is commonly applied to find the conversion function based on various mathematical models presented by several authors (da Silva et al., 2018; Jeguirim et al., 2014; Hu et al., 2016). Among these conversion functions there are the first and n^{th} order (F1), one-dimensional diffusion (D1), Two-dimensional diffusion (D2), Three-dimensional diffusion (D3), and Three-dimensional diffusion Ginstling-Brounshtein (D4).

Afterward, others complex reaction mechanisms were proposed, such as, consecutive reactions and independent parallel reactions mechanism (IPRS), since the solution obtained through global reaction was not accurate enough. which showed to be describe the pyrolysis behavior on a more reliable way. This paper focus on the parallel-reaction scheme, in which the main idea, is to separate the global reaction into individual reactions, analyze each of them and consider its fraction in the whole reaction adding the obtained result of each reaction, resulting in the global reaction model (Yu et al., 2015). The most common practice in biomass analysis is to divide the reaction into the main lignocellulosic components, which are hemicellulose, cellulose and lignin (Santos et

al., 2012; Kong et al., 2014; Rueda-Ordonez et al., 2015; Sfakiotakis & Vamvuka, 2015; Yu et al.,2015;).

Previous studies about the EFB kinetics have been developed, Nyakuma et al. (2015), studied the thermal behavior of empty fruit bunch pellets by using the Flynn-Wall-Ozawa model using heating rates of 5°C/min, 10°C/min, 20°C/min. A resulting activation energy of 160.20 KJ/mol, the results also concluded that the oil palm EFB pellets can be used as a potential material for pyrolysis. Also, Lee et al., (2017) studied the oil palm empty fruit bunch, the kernel shell, and the palm oil sludge kinetics behavior at the heating rates of 10°C/min, 20°C/min, and 40°C/min, the kinetic analysis was done by KAS and FWO models, the research showed that the EFB and PKS had a higher potential as a bio-char source. It is important to mention that no previous available works were found in the literature about kinetic analysis of the EFB blend with the PKS or about the kinetic analysis by IPRS approach of the worked biomasses in this work.

3.2 Materials and Methods

3.2.1 Biomass preparation and characterization.

The empty fruit brunch sample and the palm kernel shell were analyzed as received from a farm located in Puerto Wilches, Colombia. Due these residues in the farm were kept at ambient air, it contributed to decrease its natural moisture. These biomasses were ground and sieved to a particle size of 250 μm and the mixture samples among the biomass were made at 50 percent of mass.

The proximate analysis was made following the standards ASTM E871-82 for the moisture content (*M*), ASTM E1755-01 for the ash content (*Ash*), ASTM E872-82 for the volatile content (*VM*) and fixed carbon (*FC*) was calculated by difference on dry basis. In

order to determinate the elemental composition was used the (Parikh et al., 2007) correlations given by Eq. (1), (2) and (3) that depend mainly of the proximate analysis, in which C, H and O are the percent of carbon, hydrogen and oxygen respectively.

$$C=0.637FC+0.455VM \quad (1)$$

$$H=0.052FC+0.062VM \quad (2)$$

$$O=0.304FC+0.476VM \quad (3)$$

The higher heating value (*HHV*) was obtained following the standard ASTM D240-09 and using an oxygen calorimetric bomb IKA C200. The Eq. (4) was used to find the lower heating value (*LHV*) out (Monir et al., 2018).

$$\mathrm{LHV} = \mathrm{HHV} - 2.260\left(\frac{9\mathrm{H}}{100} + \frac{\mathrm{M}}{100}\right) \quad (4)$$

3.2.2 Experimental set-up. A thermogravimetry analyzer NETZSCH STA 449F3 was used to perform the thermal decomposition analysis. The sample mass loss was measured from room temperature up to 700°C using four different heating rates 1.25 °C/min, 2.5 °C/min, 5 °C/min, and 10 °C/min. In each experiment, the initial sample mass was around 7 mg and the sample mass loss was recorded in steps of 5 seconds or 12 measurements/min. The thermal analysis was carried out after emptied the thermogravimetric analyzer with a vacuum pump (exclusion of oxygen traces) and dried the samples, and using an argon inert atmosphere with a flow rate of 50 mL/min.

3.2.3 Kinetic Study. The kinetic analysis of thermal decomposition can be established based on the thermogravimetric data (TG) and its derivative (DTG). In order to study the TGA, it is necessary to normalize the data using Eq. (5), in which, $\boldsymbol{m_i}$ is the initial mass, *m* is the mass at time *t* and *W* is the normalized mass (Yu et al., 2018).

$$W = \frac{m}{m_i} \tag{5}$$

Also, it is necessary to normalize the DTG using Eq. (6), in which, dm⁄dt represent the DTG and *dW/dt* is the normalized DTG.

$$\frac{dW}{dt} = \frac{dm}{dt}\frac{1}{m_i} \tag{6}$$

The biomass conversion, α_e, and conversion rate, $(d\alpha/dt)_e$, are determined from the mass change, which can be calculated by Eqs. (7) and (8), respectively. In which, W_i, W and W_f are the normalized mass at the beginning, at the time *t* and at the end of the decomposition range.

$$\alpha_e = \frac{W_i - W}{W_i - W_f} \tag{7}$$

$$\left(\frac{d\alpha}{dt}\right)_e = -\frac{dW}{dt}\frac{1}{(W_i - W_f)} \tag{8}$$

The Arrhenius equation describes the solid-state theoretical conversion rate assuming that conversion of raw material into product is a single step process, and it is given by Eq. (9), in which, *E* is the activation energy (kJ⁄mol), *A* is the pre-exponential factor which represents the vibration frequency by the reaction, *β* is the heating rate, *R* is the universal gas constant (kJ⁄(mol)), *T* is the absolute temperature, and *f(α)* is the conversion function

depending on the conversion (α), the reactive concentrations and reaction order and according to the reaction mechanism proposed in this work.

$$\left(\frac{d\alpha}{dT}\right)_t = \frac{A}{\beta} \cdot [f(\alpha)] \cdot \left[exp\left(-\frac{E}{RT}\right)\right] \quad (9)$$

- ***Iso-conversion methods.*** The biomass thermal decomposition kinetics is represented by a complex mechanism of several parallel and consecutive reactions. However, in iso-conversion methods is assumed a one step-model reaction, i.e., the thermal decomposition occurs in a single step. The Vyazovkin method and the Friedman method were applied. The kinetic analysis was carried out using four heating rates, 1.25°C/min, 2.5 °C/min, 5 °C/min, and 10 °C/min. Besides, 19 conversion levels were defined from 0.05 to 0.95 with a step of 0.05.

➢ *Friedman method.* Iso-conversion differential method or Friedman method derive from taking natural logarithm for both sides in the equation of Arrhenius, Eq. (9), giving the Eq. (10).

$$\ln\left(\frac{d\alpha}{dt}\right) = \ln(A) + \ln[f(\alpha)] - \left(\frac{E}{RT}\right) \quad (10)$$

Thus, in order to find the activation energy, for each conversion level it was plotted the curve *ln(dα/dt)* as a function of *1/T*, and the slope of the straight line formed at each conversion level was multiplied by *R*, providing the activation energy.

➢ *Vyazovkin method.* All the integral methods part from the Eq. (11) where $g(\alpha)_t$ is the integrated form of the conversion function is *f(α)*.

$$g(\alpha)_t = \int \frac{1}{f(\alpha)}\ d\alpha = \frac{AE}{R\beta}\left\{-\left[\frac{\exp(x)}{x}\right] + \int_{-\infty}^{x}\left[\frac{\exp(x)}{x}\right]dx\right\} = \frac{AE}{R\beta}\ p(x) \qquad (11)$$

Eq. (11) represents the proximate solution of Eq. (9) by integration, since no analytical solutions exist. In order to solve the integral temperature in the Eq. (11) was applied an 8th degree rational approximation developed by Pérez-Maqueda & Criado, (2000) presented as Eq. (12) and considering *x =E/RT*.

$$\boldsymbol{p(x) = \left(\frac{exp(-x)}{x}\right) \cdot \left(\frac{x^7+70x^6+1886x^5 24920x^4+170136x^3+577584x^2+844560x+357120}{x^8+72x^7+2024x^6+28560x^5+216720x^4+880320x^3+1794240x^2+1572480x+403200}\right)} \qquad (12)$$

The nonlinear Vyazovkin method is presented in Eq. (13), where $\mathrm{I}\left(E_\alpha, T_i(t_\alpha)\right)_\alpha = P(x)(E_\alpha/R)$ and apparent activation energy value E_a at a given conversion degree is the value that minimizes ∅ (Jankovic, 2008).

$$\emptyset = \sum_{i}^{n}\sum_{j\neq i}^{n}\frac{\boldsymbol{I\left(E_\alpha, T_i(t_\alpha)\right)\cdot\beta_j}}{\boldsymbol{I\left(E_\alpha, T_j(t_\alpha)\right)\cdot\beta_i}} \qquad (13)$$

In this work were used four heating rates $\beta_1 = 1.25\ ℃/min$, $\beta_2 = 2.5\ ℃/min$, $\beta_3 = 5\ ℃/min$ and $\beta_4 = 10\ ℃/min$ and therefore, Eq. (13) can be rearranged as Eq. (14).

$$\emptyset = \frac{I(E_\alpha,T(t_\alpha))_{\beta_1}\cdot\beta_2}{I(E_\alpha,T(t_\alpha))_{\beta_2}\cdot\beta_1} + \frac{I(E_\alpha,T(t_\alpha))_{\beta_1}\cdot\beta_3}{I(E_\alpha,T(t_\alpha))_{\beta_3}\cdot\beta_1} + \frac{I(E_\alpha,T(t_\alpha))_{\beta_1}\cdot\beta_4}{I(E_\alpha,T(t_\alpha))_{\beta_4}\cdot\beta_1} + \frac{I(E_\alpha,T(t_\alpha))_{\beta_2}\cdot\beta_1}{I(E_\alpha,T(t_\alpha))_{\beta_1}*\beta_2} + \frac{I(E_\alpha,T(t_\alpha))_{\beta_2}\cdot\beta_3}{I(E_\alpha,T(t_\alpha))_{\beta_3}\cdot\beta_2} +$$

$$\frac{I(E_\alpha,T(t_\alpha))_{\beta_2}\cdot\beta_4}{I(E_\alpha,T(t_\alpha))_{\beta_4}\cdot\beta_2} + \frac{I(E_\alpha,T(t_\alpha))_{\beta_3}\cdot\beta_1}{I(E_\alpha,T(t_\alpha))_{\beta_1}\cdot\beta_3} + \frac{I(E_\alpha,T(t_\alpha))_{\beta_3}\cdot\beta_2}{I(E_\alpha,T(t_\alpha))_{\beta_2}\cdot\beta_3} + \frac{I(E_\alpha,T(t_\alpha))_{\beta_3}\cdot\beta_4}{I(E_\alpha,T(t_\alpha))_{\beta_4}\cdot\beta_3} + \frac{I(E_\alpha,T(t_\alpha))_{\beta_4}\cdot\beta_1}{I(E_\alpha,T(t_\alpha))_{\beta_1}\cdot\beta_4} +$$

$$\frac{I(E_\alpha,T(t_\alpha))_{\beta_4}\cdot\beta_2}{I(E_\alpha,T(t_\alpha))_{\beta_2}\cdot\beta_4} + \frac{I(E_\alpha,T(t_\alpha))_{\beta_4}\cdot\beta_3}{I(E_\alpha,T(t_\alpha))_{\beta_3}\cdot\beta_4} \qquad (14)$$

- *Determination of the conversion function.* The evaluation of Eq. (11) in the conversion level of 50 %, allows obtaining Eq. (15), in which $x_{0.5} = E_a/RT_{0.5}$ and $T_{0.5}$ is the temperature in that conversion level.

$$g(0.5) = \frac{A \cdot E_a}{\beta \cdot R} p(x_{0.5}) \tag{15}$$

The influence of the pre-exponential factor is eliminated dividing the Eq. (11) by the Eq. (15) obtaining Eq. (16), in which, $g(x)/g(x_{0.5})$ represents the theoretical Master Plot and $p(x)/p(x_{0.5})$ represents the experimental Master Plot.

$$\frac{g(\alpha)}{g(0.5)} = \frac{\frac{A \cdot E_a}{\beta \cdot R} p(x)}{\frac{A \cdot E_a}{\beta \cdot R} p(x_{0.5})} = \frac{p(x)}{p(x_{0.5})} \tag{16}$$

- *Pre-exponential factor formulation.* In order to calculate the pre-exponential factor, Eq. (9) was rearranged by linearization, obtaining Eq. (17) and plotted $ln[(d\alpha/dt)/f(\alpha)]$ as function of 1/T.

$$ln\left[\frac{(d\alpha/dt)}{f(\alpha)}\right] = ln(A) - \frac{E}{R \cdot T} \tag{17}$$

Through a linear regression of the plotted data, in which the intersection with the axis Y represents the pre-exponential factor natural logarithm, and the linear regression slope multiplied by the universal gas constant is the activation energy. This activation energy should not differ more than 10% from the values provided by Friedman method (Rueda-Ordóñez & Tannous, 2015).

- ***Mechanism of Independent parallel-reaction.*** The independent parallel reactions mechanism is showed in Eq. (18), where F_i volatile mass fraction is related with each pseudo component and n is the assumed reaction number.

$$\frac{d\alpha}{dt} = \sum_{i}^{n} F_i \frac{d\alpha_i}{dt} = \sum_{i}^{n} F_i A_i \exp\left(-\frac{E_i}{RT}\right) f(\alpha_i) \tag{18}$$

Rearranging Eq. (18) for this work into Eq. (19), where *HC*, *C* and *L* are volatile mass fraction related with the hemicellulose, cellulose, and lignin, respectively.

$$\frac{d\alpha}{dt} = HC\left(\frac{d\alpha}{dt}\right)_{HC} + C\left(\frac{d\alpha}{dt}\right)_{C} + L\left(\frac{d\alpha}{dt}\right)_{L} \tag{19}$$

In order to obtain the theoretical conversion for the solution of Eq. (9) and Eq. (18), the temperature was controlled by Eq. (20), in which T_0=150 °C, corresponding to the beginning of the thermal decomposition and the end of the drying stage. Also, β represent the heating rate (°C/s), and *t* (s) the time, following Eq. (21), in which t_0 was the time at 150 °C and *h* the step selected (5 s).

$$T = T_0 + \beta t \tag{20}$$

$$t = t_0 + h \tag{21}$$

Finally, the solution of the theoretical conversion, and the determination of the kinetic parameters in the independent parallel reactions mechanism were carried out applying the first order Euler method, and the obtained curve was fitted to the experimental data by the least squares method. The quality of fit was measured with the average deviation (*AD*) presented in Eq. (22), and was applied a reliability criterion of *AD* < 3%. In Eq. (22), $(d\alpha/dt)_{e,max}$ is the maximum experimental conversion rate, *e* and *t* are experimental and theoretical data, and *N* the number of experimental points considered were 9408, 4704, 2352 and 1176 for 1.25 °C/min, 2.5 °C/min, 5 °C/min, and 10 °C/min, respectively.

$$\boldsymbol{Error\ porcentage}(\%) = \left[\frac{\sqrt{\frac{\sum_{i=0}^{N}\left[(\boldsymbol{y})_{experimental} - (\boldsymbol{y})_{theoretical}\right]^2}{\boldsymbol{N}}}}{(\boldsymbol{y})_{experimental,maximum}}\right]\mathbf{100} \quad (22)$$

When $\boldsymbol{y} = \frac{\boldsymbol{d\alpha}}{\boldsymbol{dt}}$, the error percentage will be denoted as AD.
When $\boldsymbol{y} = \boldsymbol{\alpha}$, the error percentage will be called AVP.

3.3 Result and analysis

3.3.1 Biomass characterization. The EFB, PKS and blend characterization is shown in the table 8, the obtained values for the proximate, ultimate and heating value are presented as well as the review from previous authors, which shows that the obtained values for the different analyzes presented followed the expected behavior according to the found literature. (Abdullah & Gerhauser, 2008; Chew et al.,2016; Lee et al., 2017). Except for the results obtained by Chew et al., (2016), which significantly differs in the *VM*, *FC* and *HHV*, tending to a different behavior from the evidenced in table 8.

On the other hand, the blend properties evidenced an intermediate behavior, but presenting a tendency to be closer to the PKS sample values, except for moisture that presented a higher value than the two samples, and the fixed carbon that had the same value of the palm kernel shell.

Table 8.
physical-chemical properties of the EFB, PKS and its blend.

Author	This work	This work	This work	Abdullah & Gerhauser (2008)	Chew et al. (2016)	Lee et al. (2017)
(Material)	EFB	Blend	PKS	EFB	EFB	EFB
Proximate analysis (%) Dry basis						
M	6.43 ± 0.23	7.17 ± 0.24	6.28	7.95	7.16	3.47
Ash	8.19 ± 0.036	5.43 ± 0.05	3.74	5.36	6.96	11.10
VM	78.92 ± 0.30	83.68 ± 0.56	85.38	83.86	68.58	72.88
FC	12.88	10.89	10.89	10.78	17.30	12.56
Ultimate analysis (%) Dry basis						
C	44.12	45.01	45.78	49.07	44.8	50.89
H	5.56	5.75	5.86	6.45	7.30	-
O	41.48	43.14	43.95	38.29	46.78	42.44
Heating Value (MJ/Kg) Dry basis						
HHV	19.71	19.97 ± 0.21	20.22	19.35	17.94	19.65
LHV	18.43	18.63	18.89	-	-	-

3.3.2 Thermal decomposition. Fig.7 present the TG and DTG curves of thermal decomposition process of the EFB, the blend and PKS in inert atmosphere of argon at the studied heating rates. Table 9 presents the most significate thermal decomposition stages: volatile release and carbonization. The dehydration stage is not taken into account because the samples were dried before each analysis. In the temperature range between 150 and 200 °C, the mass variation was lower than 5% for all biomass, and was related to the evaporation of some extractives in the biomass, and in this work, the effect of this process was considered negligible.

- ***Volatile release.*** This stage corresponds to the temperature range of 200 – 400°C and it is related to the main mass loss in the thermal decomposition process. According to the Table 9, the blend presents the higher mass loss, 61.22%, the heating rate of 10°C/min and the EFB present the lower weight loss, 56.10%, at the heating rate of 1.25°C/min. The behavior among the different biomass is similar in this stage.

The Fig 7(b) present the EBF DTG curve; there is just a major peak that can be related mainly with the thermal decomposition of the hemicellulose and cellulose maximum decomposition rate at 277.7°C, 288.8°C, 295.7°C and 306.8°C for the related heating rates, respectively. In other matters, the Fig 7 (d) present the blend DTG; in which the major peak was related to the cellulose maximum decomposition rate at 286.3°C, 297.8°C, 308.2°C and 312.5°C for the implemented heating rates, respectively. Furthermore, there is shoulder that correspond to the hemicellulose decomposition at 238.5°C, 248°C, 260.8°C and 265.3°C for the heating rates evaluated, respectively. On the other hand, the Fig 7 (f) presents the PKS DTG; and is observed that there are two major peaks in this zone, the first peak is related with the hemicellulose maximum decomposition rate at 252°C, 260°C, 270°C and 276°C for the heating rates evaluated, respectively. The second peak, corresponds to the cellulose maximum decomposition rate at 314°C, 325°C, 333°C and 345°C for the related heating rates, respectively.

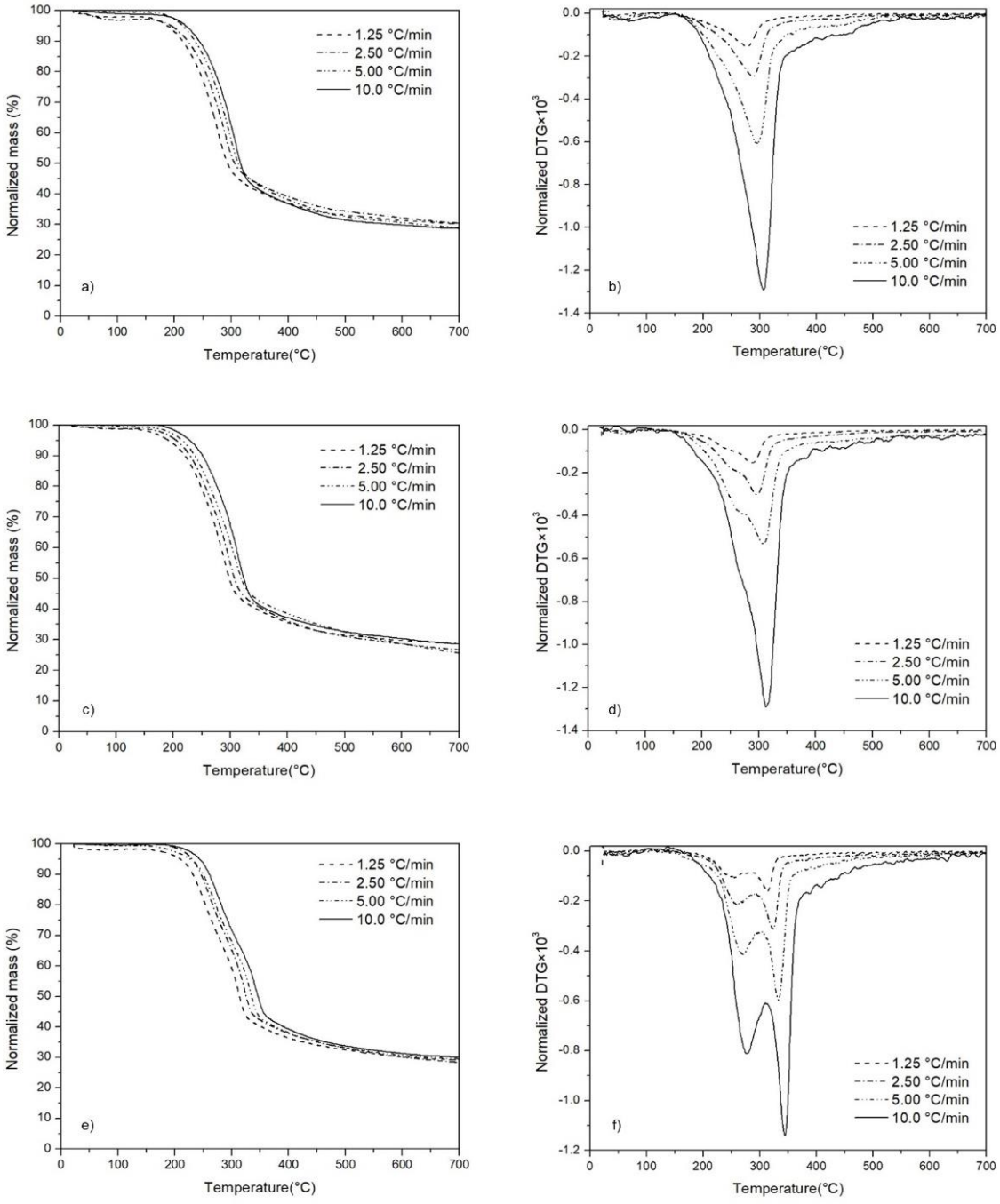

Figure 7. *(a) TG EBF, (b) DTG EBF, (c) TG Blend, (d) DTG Blend, (e) TG PKS, and (f) DTG PKS.*

Table 9.
Normalized mass variation trough thermal decomposition stages.

Δ Normalized mass (%)				
β (°C/min)	**1.25**	**2.5**	**5**	**10**
EFB				
Volatile release	56.10	55.31	59.12	60.69
Carbonization	6.88	8.64	9.20	8.05
Blend				
Volatile release	58.34	59.60	58.55	61.22
Carbonization	6.95	9.48	12.92	8.64
PKS				
Volatile release	59.62	60.95	59.33	59.90
Carbonization	7.26	9.50	8.59	9.19

- ***Carbonization.*** This phase corresponds to the temperature range of 400 – 700°C and it is related only to the thermal decomposition of lignin. The blend presents the higher weight loss, 12.92%, at the heating rate of 5°C/min, and the EFB present the lower mass loss, 6.88%, at the heating rate of 1.25°C/min.

Bio-char and ashes mainly compose the result of this stage at 700°C. Excluding the ash percentage, The EFB present 21.96%, 22.21%, 20.7% and 20.49% of bio-char for the heating rates evaluated, respectively. The blend present 23.19%, 21.2%, 20.13% and 23.08% of bio-char for the implemented heating rates, respectively. The PKS present 25.36%, 24.60%, 25.75% and 26.34% of bio-char for the related heating rates, respectively.

3.3.3 Kinetic modelling.

- ***Activation energy calculation through Isoconversional analysis.*** Table 10 summarizes the results of the kinetic analysis as a single global reaction for the EFB and its blend with PKS. It is important to mention that according to Vyazovkin et al., (2011) in the ICTAC meeting, when a difference in the activation energies values is higher than 20-30% of the average *Ea*, then, the reaction obeys to a complex pathway. Therefore, for such reason one global reaction scheme may not be accurate enough for describing the thermal decomposition behavior, thus, more complex methods must be implemented.

Table 10.
Isoconversional Model kinetic parameters and validation for the EFB, PKS and Blend.

Single global step model kinetic results			
(Material)	EFB	PKS Blend	PKS
f(α)	D3	D3	D3
Ea (kJ/mol)	171.14	163.11	145.21
E_F (kJ/mol)	143.21 - 260.60	138.45 - 220.40	168.71 - 191.50
$\bar{E}_{aF}$ (kJ/mol)	197.52	191.09	180.13
E_v (kJ/mol)	120.50 - 227.30	114.55 - 178.59	152.70 - 182.55
$\bar{E}_{av}$ (kJ/mol)	180.90	178.59	178.24
$\log_{10}(A)$ (Log_{10} (S^{-1}))	12.62	11.73	9.48

Ea: Activation energy.
Ev: Apparent activation energy by Vyazovkin method.
$\bar{E}$av: Average apparent activation energy by Friedman method.
$\bar{E}_{aF:}$ Average apparent activation energy by Friedman method.
Ef: Apparent activation energy by Friedman method.

From table 10, the EFB apparent activation energy by Friedman method presented a 62.47% of difference between the minimum and maximum value, on the other hand, the Vyazovkin method presented a 59.04% of difference of the average. Also, the blend with the PKS, presents a difference between the minimum and the maximum of 42.88% and 53.22% of the average activation energy by FD and VZ methods respectively.

Fig. 8 (a) and (b) presents the behavior of the activation energy as a function of conversion, for both EFB and its blend, which showed, that the activation energies estimated by Friedman model are higher than those obtained by Vyazovkin method, this could be explained since, the two methods have a different mathematic base.

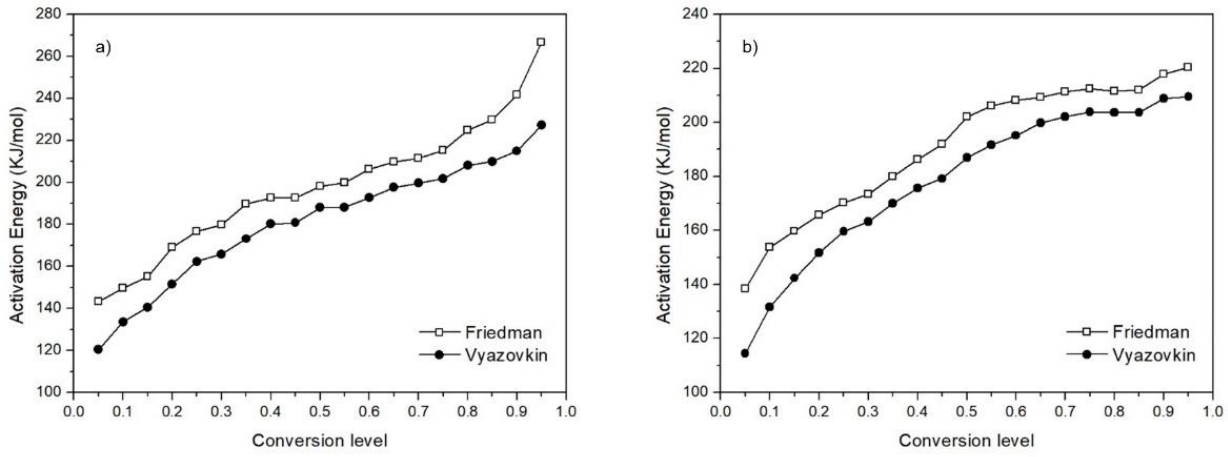

Figure 8. Activation energy as a function of conversion by Friedman and Vyazovkin iso-conversion mechanisms. (a) EFB and (b) Blend.

- ***Reaction mechanism and pre-exponential factor calculation.*** Fig. 9 and Table 11 presents the master plots comparison for both the empty fruit bunch and the blend with kernel shell, from the obtained behavior, it is evidenced that the reaction mechanism that better fitted was the three-dimensional diffusion (D3). Also, is observed that the reaction mechanism for the palm kernel shell was also represented by the previously mentioned mechanism.

Table 11.

Comparison between chemical reaction models and heating rates by AVP.

Symbol	$f(\alpha)$	EFB (%)	Blend (%)
F1	$(1-\alpha)^n$	245.90	285.71
D1	$1/2\alpha$	253.39	292.13
D2	$\frac{1}{-ln(1-\alpha)}$	202.09	240.76
D3	$\left(\frac{1}{2}\right)\cdot\frac{3(1-\alpha)^{2/3}}{1-(1-\alpha)^{1/3}}$	91.03	131.65
D4	$\left(\frac{1}{2}\right)\cdot\frac{3}{(1-\alpha)^{-1/3}-1}$	170.61	209.52

Afterwards by using the pre-exponential factor for both samples was calculated as a linearization of the *ln(dα/dt)/f(α)* as a function *1/T*. For the EFB, the resulting function was ln(dα/dt)/f(α)= -20.58(1/T) + 29.07, with a coefficient of determination, R^2=0.9999. Therefore, the logarithm of the pre-exponential factor of 12.62 was obtained, this is presented in Fig. 10, subsequently, by multiplying the function slope by the ideal gas constant (8,314 J/mol K), the final activation energy of the kinetic model was calculated, providing a value of 178.59 kJ/mol. Besides, for the blend, the linearization equation was

ln(dα/dt)/f(α)= -19.62(1/T) + 27.00, thus, the logarithm of the pre-exponential factor was 11.73, and the final activation energy was 163.11 kJ/mol.

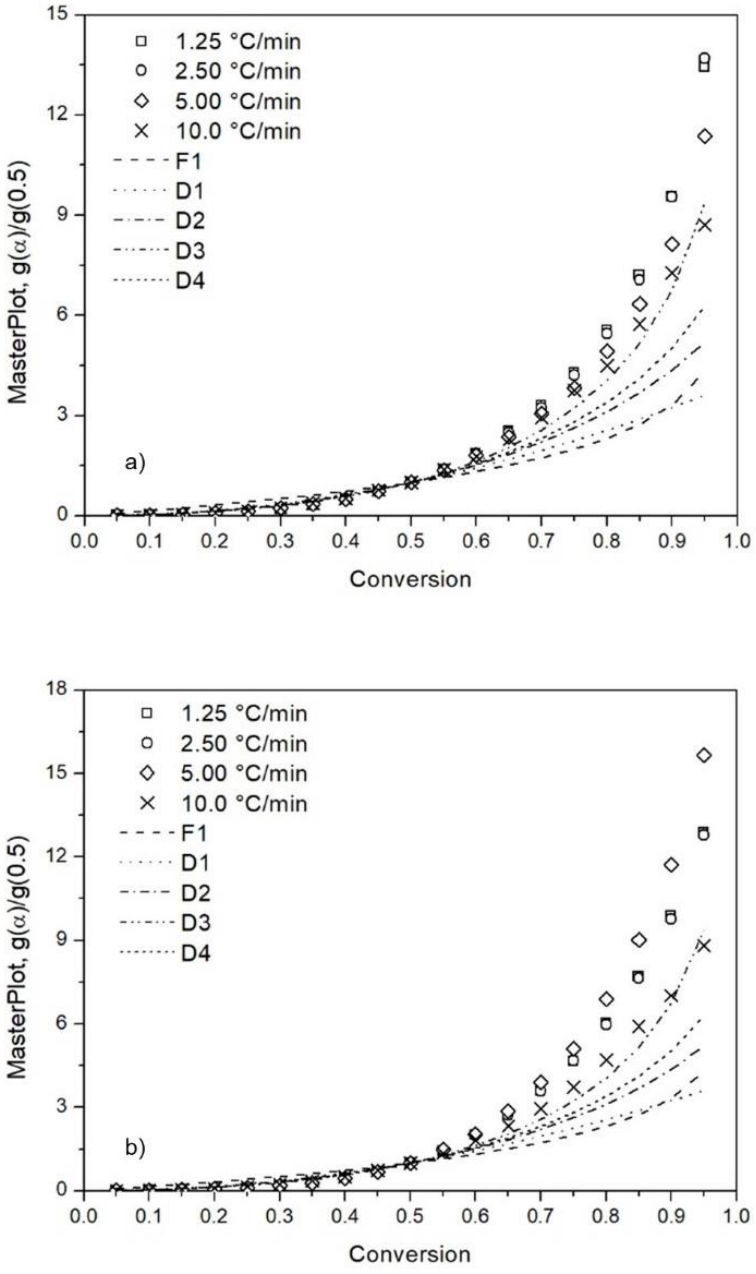

Figure 9. *Master plots results (a) for EFB and (b) for the blend between EFB and KS*

Fig. 11 shows the normalized conversion, α, against temperature, T, in which the solid lines were obtained with the kinetic parameters presented previously in Table 10, for both EFB and the blend with PKS. The comparison between theoretical and experimental data shows an error of less than 4% for both models. Nevertheless, even validated through statistics, results were not considered be accurate enough, but even if it is validated through statistics, as presented in table 12, it would not be accurate enough, since the activation energy behavior presented a high difference, not following the recommendations mentioned by Vyazovkin et al., (2011).

Table 12.

Iso-conversion model validation.

	EFB				
B °C/min	**1.25**	**2.5**	**5**	**10**	**Average**
Error (AVP)%	2.22	2.93	1.41	2.69	2.31
	BLEND				
B °C/min	**1.25**	**2.5**	**5**	**10**	**Average**
Error (AVP)%	3.51	2.49	2.2	2.45	2.66

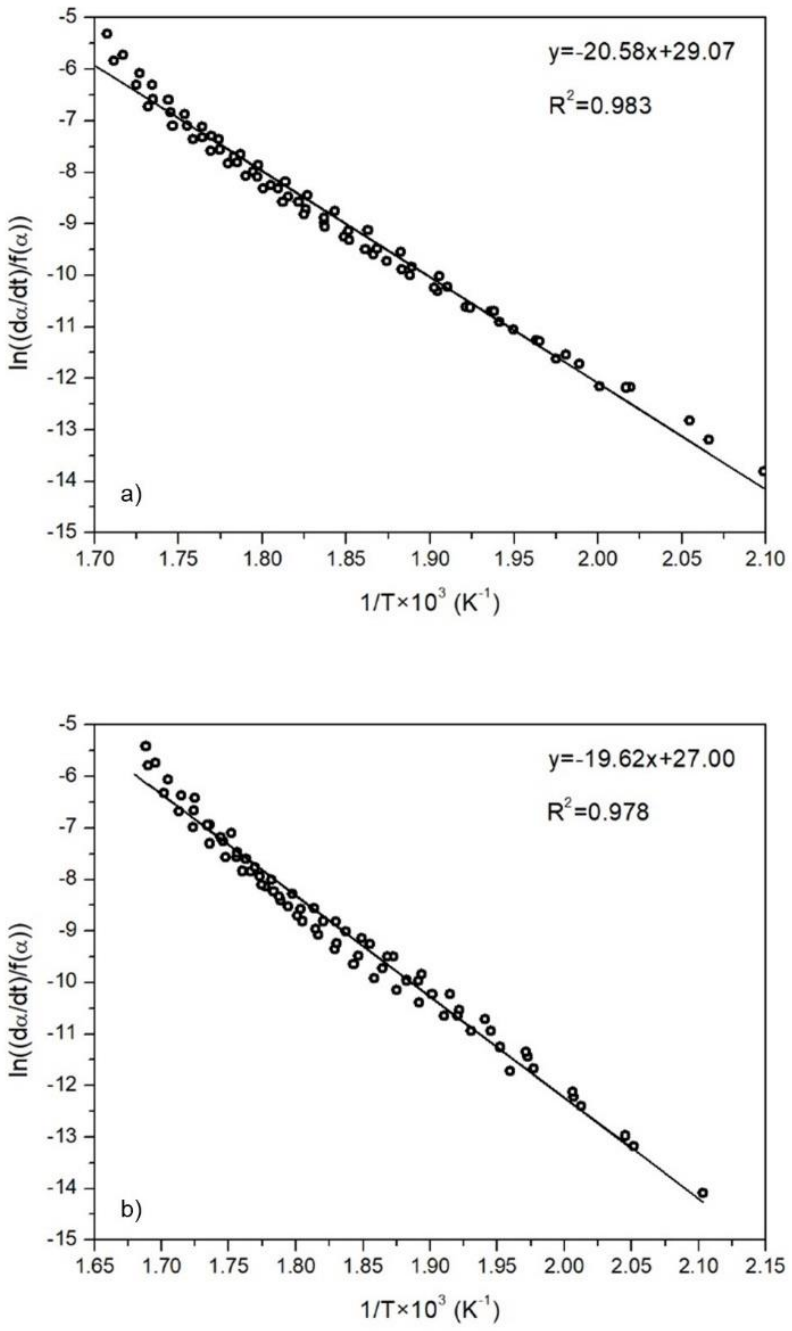

Figure 10. Linearization result of the ln(dα/dt)/f(α) as a function of 1/T (a) EFB and (b) the Blend.

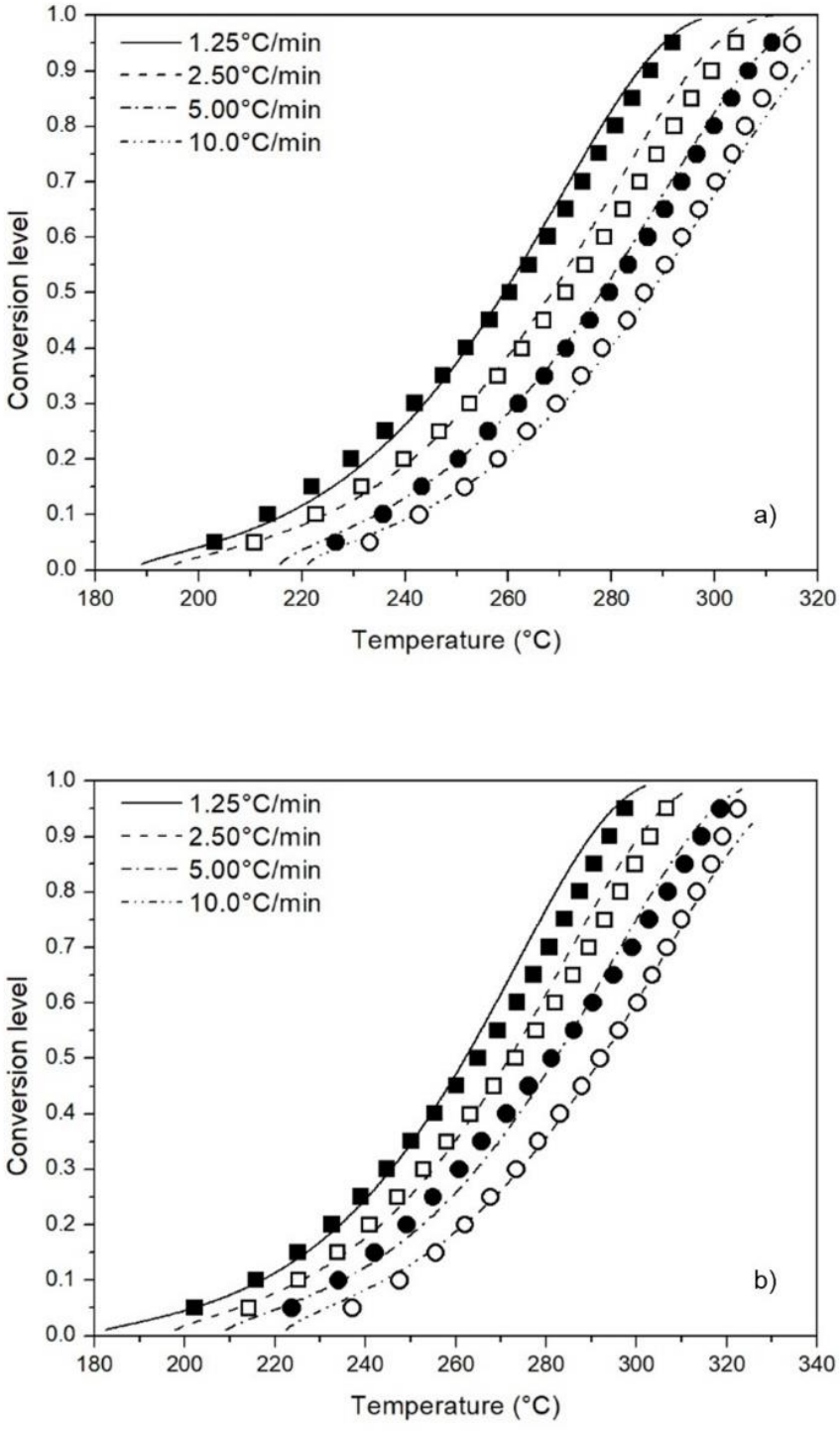

Figure 11. Conversion as a function of temperature for (a) EFB and (b) the blend level.

3.3.4 Independent parallel-reaction mechanism. As previously discussed, the kinetic triplet obtained by one global reaction did not give an accurate answer modelling the thermal behavior of the EFB and the blend, thus, IPRS methodology was considered. Table 13 summarizes the resulting kinetic parameters assuming a three-parallel reaction scheme for the studied samples. From the obtained values, it is possible to observe that the kinetic parameters of the blend did not obey an intermediate behavior with the EFB and the PKS, since none of the obtained parameters were in between the kernel shell or the empty fruit bunch results, except for the composition fraction.

Table 13.

IPRS Kinetic parameters for each of the studied samples.

EFB			
	R1 (HC)	**R2 (C)**	**R3 (L)**
$f(\alpha)$	$(1-\alpha)^n$	$(1-\alpha)^n$	$(1-\alpha)^n$
n	1	1	2.9
E (kJ/mol)	80.40± 1.23	181.50±0.50	29.60±1.04
Log10(*A*) ($Log_{10}(S^{-1})$)	4.99±0.12	13.96±0.03	-0.87±0.31
F	0.25±0.05	0.24±0.04	0.51±0.09
BLEND			
	R1 (HC)	**R2 (C)**	**R3 (L)**
$f(\alpha)$	$(1-\alpha)^n$	$(1-\alpha)^n$	$(1-\alpha)^n$
n	1	1	2.5
E (kJ/mol)	112.33± 0.58	221.17±0.76	29.00±1.00
Log10(*A*) ($Log_{10}(S^{-1})$)	7.97±0.06	16.53±0.06	-0.92±0.23
F	0.27±0.03	0.28±0.01	0.45±0.03
PKS			
	R1 (HC)	**R2 (C)**	**R3 (L)**
$f(\alpha)$	$(1-\alpha)^n$	$(1-\alpha)^n$	$(1-\alpha)^n$
n	1	1	1.75
E (kJ/mol)	106.75	186.25	31.33
Log10(*A*) ($Log_{10}(S^{-1})$)	7.71	13.86	-0.73
F	0.32	0.33	0.35

Fig. 12 presents the obtained behavior for each of the analyzed samples at the studied heating rates, the EFB lignocellulosic components reactions occurred in the intervals of temperatures of 150 to 340 °C for hemicellulose, 200 to 350°C for cellulose, and 100 to 700 for lignin. Therefore, followed the behavior expected for the lignocellulosic components according to different authors (Yang et al., 2007; Liu et al., 2011; Cai et al., 2013; Rueda-Ordoñez & Tannous, 2015).

Fig. 13 illustrates the behavior of the blend with the PKS, the results shows that the EFB is dominant in the reaction since the kinetic behavior is similar to the presented in Fig. 12. The temperature intervals of reaction for the HC, C and lignin, were varied from 150 to 340°C, 210 to 350°C, and from 100 to 700°C for the mentioned components respectively, also following the previous mentioned literature. As it was mentioned previously in the DTG results discussion, the evidenced shoulder in the blend kinetic behavior is explained with the hemicellulose reaction, which is also, the more significative effect of the PKS in the global behavior.

Table 14 presents the statistical validation of the modelling results by average deviation AD and AVP, a deviation of less than 4% was accomplished for both samples, thus, meaning that the models correctly represented the thermal decomposition behavior.

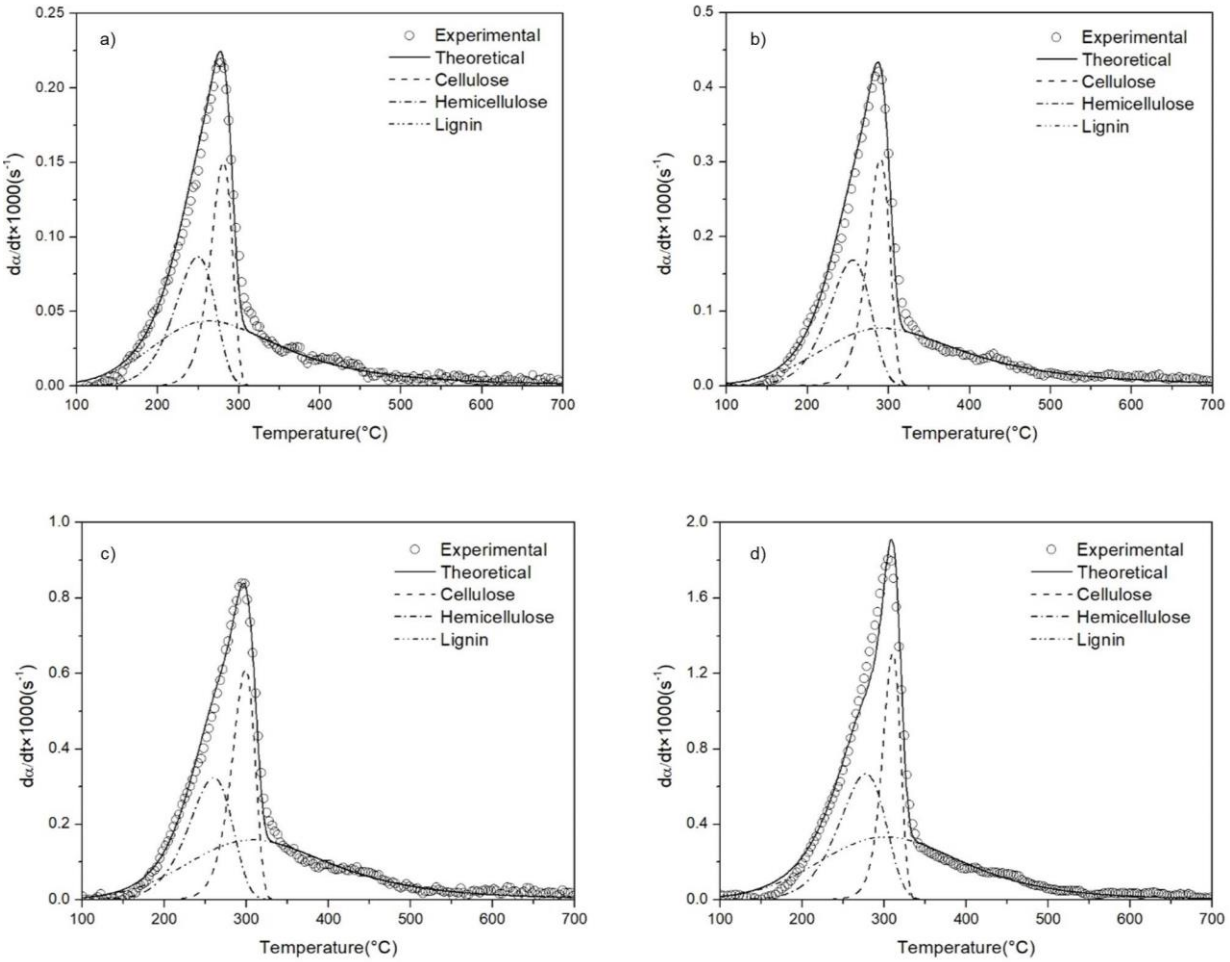

Figure 12. IPRS result of the EFB at the heating rates of (a) 1.25°C/min (b) 2.5 °C/min (c) 5.0 °C/min and (d) 10°C/min.

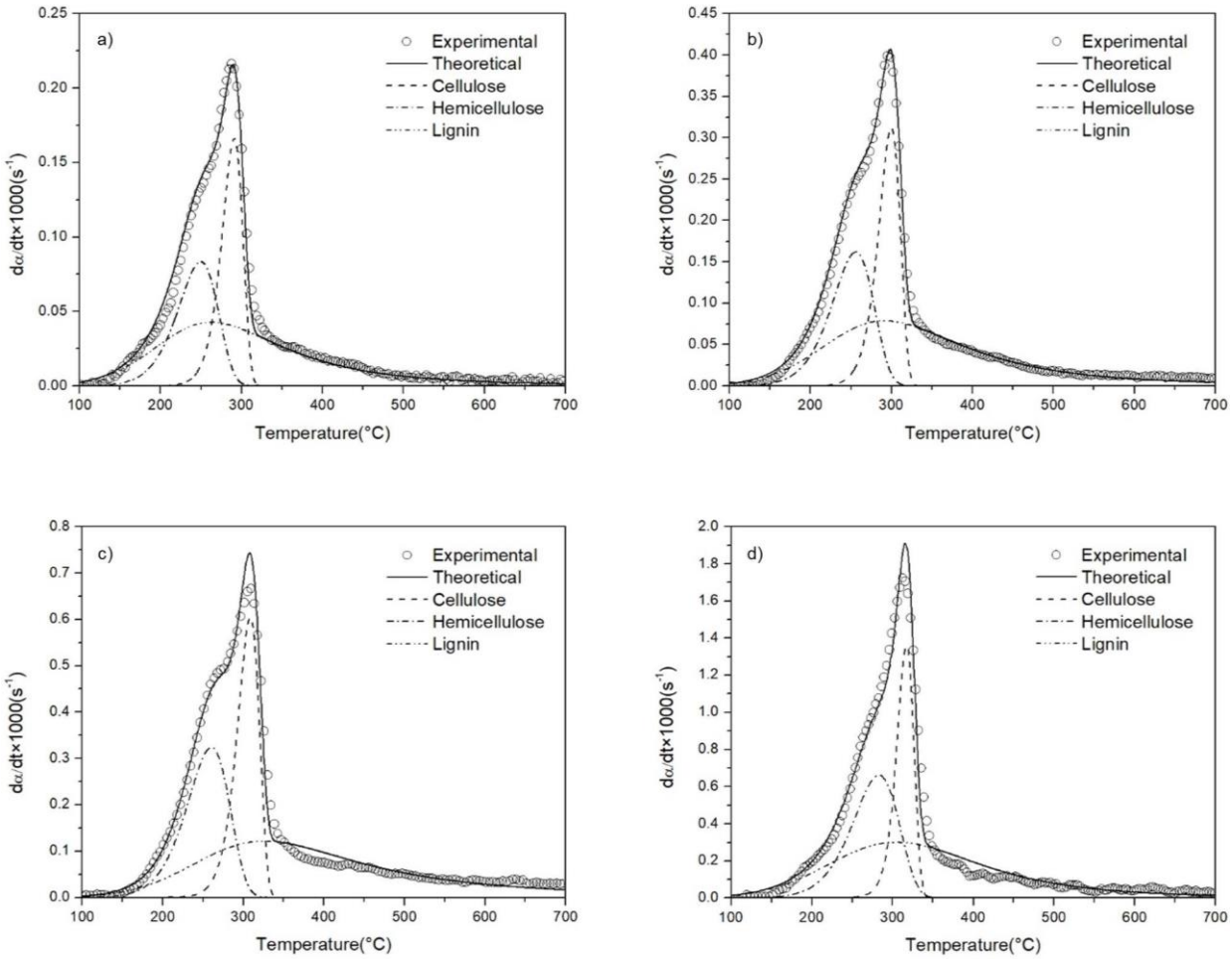

Figure 13. IPRS results of the biomass blend at the heating rates of (a) 1.25°C/min (b) 2.5 °C/min (c) 5.0 °C/min and (d) 10°C/min.

Table 14.

IPRS models' validation by average deviation criteria for the EFB and the blend.

EFB					
B °C/min	**1.25**	**2.5**	**5**	**10**	**Average**
Error (AD)%	2.86	2.65	2.08	2.87	2.53
Error (AVP)%	2.76	2.99	1.78	2.55	2.51
BLEND					
B °C/min	**1.25**	**2.5**	**5**	**10**	**Average**
Error (AD)%	2.32	1.6	2.99	3.36	2.3
Error (AVP)%	2.14	2.92	1.68	2.85	2.25

3.4 Conclusion

Due to the thermal characteristics (high content of ashes), the empty fruit brunch is not good as raw material for the pyrolysis process but the behavior it is enhanced significantly with the blend with palm kernel shell, though the EFB might be still useful for other thermo-chemical processes such as the gasification, in which the ashes are desirable. The thermal decomposition was described by isoconversional methods with a good accuracy and fitting, but due to the variation of the activation energy along the conversion the behavior obeys a multistep reaction pathway. Additionally, the thermal decomposition of both biomass was modeled accurately with a three-independent parallel reaction mechanism; the error was less 4% by average deviation criteria.

3.5 References

Abdullah, N., & Gerhauser, H. (2008). Bio-oil derived from empty fruit bunches. *Fuel*, *87*(12), 2606-2613. doi: 10.1016/j.fuel.2008.02.011

Cai, J., Wu, W., Liu, R. & Huber, G. (2013). A distributed activation energy model for the pyrolysis of lignocellulosic biomass. *Green Chemistry*, *15*(5), 1331-1340. doi: 10.1039/C3GC36958G

Chen, Z., Hu, M., Zhu, X., Guo, D., Liu, S., Hu, Z., Xiao, B., Wang, J. & Laghari, M. (2015). Characteristics and kinetic study on pyrolysis of five lignocellulosic biomass via thermogravimetric analysis. *Bioresource Technology*, *192*, 441-450. doi: 10.1016/j.biortech.2015.05.062

Chew, J., Doshi, V., Yong, S., & Bhattacharya, S. (2016). Kinetic study of torrefaction of oil palm shell, mesocarp and empty fruit bunch. *Journal Of Thermal Analysis And Calorimetry*, *126*(2), 709-715. doi:10.1007/s10973-016-5518-3

da Silva, J., Alves, J., Galdino, W., Andersen, S., & de Sena, R. (2018). Pyrolysis kinetic evaluation by single-step for waste wood from reforestation. *Waste Management*, *72*, 265-273. doi:10.1016/j.wasman.2017.11.034

Friedman, H. L. (1964). Kinetics of thermal degradation of char-forming plastics from thermogravimetry. Application to a phenolic plastic. *Journal of Polymer Science Part C: Polymer Symposia*, *6*(1), 183–195. doi: 10.1002/polc.5070060121

Hu, M., Chen, Z., Wang, S., Guo, D., Ma, C., Zhou, Y., Chen, J., Laghari, M., Fazal, S., Xiao, B., Zhang, B. & Ma, S. (2016). Thermogravimetric kinetics of lignocellulosic biomass slow pyrolysis using distributed activation energy model, Fraser–Suzuki deconvolution, and iso-conversional method. *Energy Conversion and Management*, *118*, 1-11. doi: 10.1016/j.enconman.2016.03.058

Jankovic, B. (2008). Kinetic analysis of the nonisothermal decomposition of potassium metabisulfite using the model-fitting and isoconversional (model-free) methods. *Chemical Engineering Journal*, *139*(1), 128-135. doi: 10.1016/j.cej.2007.07.085

Jeguirim, M., Bikai, J., Elmay, Y., Limousy, L. & Njeugna, E. (2014). Thermal characterization and pyrolysis kinetics of tropical biomass feedstocks for energy recovery. *Energy for Sustainable Development*, *23*, 188-193. doi: 10.1016/j.esd.2014.09.009

Kong, S., Loh, S., Bachmann, R., Rahim, S., & Salimon, J. (2014). Biochar from oil palm biomass: A review of its potential and challenges. *Renewable And Sustainable Energy Reviews*, *39*, 729-739. doi: 10.1016/j.rser.2014.07.107

Lee, X., Lee, L., Gan, S., Thangalazhy-Gopakumar, S., & Ng, H. (2017). Biochar potential evaluation of palm oil wastes through slow pyrolysis: Thermochemical characterization and pyrolytic kinetic studies. *Bioresource Technology*, *236*, 155-163. doi: 10.1016/j.biortech.2017.03.105

Liu, Q., Zhong, Z., Wang, S. & Luo, Z. (2011). Interactions of biomass components during pyrolysis: A TG-FTIR study. *Journal of Analytical and Applied Pyrolysis*, *90*(2), 213-218. doi:10.1016/j.jaap.2010.12.009

Mishra, R. & Mohanty, K. (2018). Pyrolysis kinetics and thermal behavior of waste sawdust biomass using thermogravimetric analysis. *Bioresource Technology*, *251*, 63-74. doi: 10.1016/j.biortech.2017.12.029

Monir, M., Abd Aziz, A., Kristanti, R., & Yousuf, A. (2018). Co-gasification of empty fruit bunch in a downdraft reactor: A pilot scale approach. *Bioresource Technology Reports*, *1*, 39-49. doi: 10.1016/j.biteb.2018.02.001

Nyakuma, B., Ahmad, A., Abdullah, T., Oladokun, O., & Aminu, D. (2015). Non-Isothermal Kinetic Analysis of Oil Palm Empty Fruit Bunch Pellets by Thermogravimetric Analysis. *Chemical Engineering Transactions*, *45*, 1327-1332. doi: 10.3303/CET1545222

Parikh, J., Channiwala, S., & Ghosal, G. (2007). A correlation for calculating elemental composition from proximate analysis of biomass materials. *Fuel*, *86*(12-13), 1710-1719. doi: 10.1016/j.fuel.2006.12.029

Pérez-Maqueda, L., & Criado, J. (2000). Journal Of Thermal Analysis And Calorimetry, *60*(3), 909-915. doi: 10.1023/a:1010115926340

Quan, C., Gao, N., & Song, Q. (2016). Pyrolysis of biomass components in a TGA and a fixed-bed reactor: Thermochemical behaviors, kinetics, and product characterization. Journal of Analytical and Applied Pyrolysis, *121*, 84-92. doi: 10.1016/j.jaap.2016.07.005

Rueda-Ordóñez, Y.J., Baroni, E.G., Tinoco-Navarro, L.K., Tannous, K. (2015). Modeling the kinetics of lignocellulosic biomass pyrolysis. In: Tannous, K. (Ed.), Innovative Solutions in Fluid-Particle Systems and Renewable Energy Management. IGI Global, Hershey, 92–130. doi:10.4018/978-1-4666-8711-0.ch004.

Rueda-Ordóñez, Y.J., Tannous, K. (2015). Isoconversional kinetic study of the thermal decomposition of sugarcane straw for thermal conversion processes. *Bioresource. Technology*. *196*, 136-144. doi: 10.1016/j.biortech.2015.07.062

Santos, K., Lobato, F., Lira, T., Murata, V., & Barrozo, M. (2012). Sensitivity analysis applied to independent parallel reaction model for pyrolysis of bagasse. *Chemical Engineering Research And Design*, *90*(11), 1989-1996. doi: 10.1016/j.cherd.2012.04.007

Vyazovkin**,** S. (2000). Modification of the integral isoconversional method to account for variation in the activation energy. *Journal of Computational Chemistry*, *22*(2), 178-183. doi: 10.1002/1096-987X(20010130)22:2<178::AID-JCC5>3.0.CO;2-#

Vyazovkin, S., Burnham, A., Criado, J., Pérez-Maqueda, L., Popescu, C., & Sbirrazzuoli, N. (2011). ICTAC Kinetics Committee recommendations for performing kinetic computations on thermal analysis data. Thermochimica Acta, *520*(1-2), 1-19. doi: 10.1016/j.tca.2011.03.034

Yu, H., Liu, F., Ke, M., & Zhang, X. (2015). Thermogravimetric analysis and kinetic study of bamboo waste treated by Echinodontium taxodii using a modified three-parallel-reactions model. *Bioresource Technology*, *185*, 324-330. doi: 10.1016/j.biortech.2015.03.005

Reference list

Abdullah, N., & Gerhauser, H. (2008). Bio-oil derived from empty fruit bunches. *Fuel*, *87*(12), 2606-2613. doi: 10.1016/j.fuel.2008.02.011

Asadullah, M., Rasid, N., Kadir, S., & Azdarpour, A. (2018). Production and detailed characterization of bio-oil from fast pyrolysis of palm kernel shell. *biomass and bioenergy*, *59*(2013) 316-324. doi: 10.1016/j.biombioe.2013.08.037

Barroso Casillas, M., (2010). pretratamiento de biomasa celulósica para la obtención de etanol en el marco de una biorrefinería. (tesis de pregrado). Universidad Politécnica de Madrid. Recuperado de: http://oa.upm.es/10559/1/MIGUEL_BARROSO_CASILLAS.pdf

Braun, R. L., Burnham, A. K., Reynolds, J. G., & Clarkson, J. E. (1991). Pyrolysis kinetics for lacustrine and marine source rocks by programmed micropyrolysis. *Energy and Fuels*, *5*(1), 192–204. doi:10.1021/ef00025a033.

Cai, J., Wu, W., Liu, R. & Huber, G. (2013). A distributed activation energy model for the pyrolysis of lignocellulosic biomass. *Green Chemistry*, *15*(5), 1331-1340. doi: 10.1039/C3GC36958G

Carreño Pineda, L., Caicedo Mesa, L., & Martínez Riascos, C., (2012). Técnicas de fermetación y aplicaciones de la celulosa bacteriana: una revisión. *Ingeniería y ciencia*, *8*(16), 307-335. Retrieved from: http://www.scielo.org.co/pdf/ince/v8n16/v8n16a12.pdf

Chan,Y.H., Quitain, A.,Yuzuo, S., Uemura, Y., Sasaki, M., & Kida, T. (2017) Liquefaction of palm kernel shell in sub- and supercritical water for bio-oil production, *Journal of the Energy Institute*, in press. doi:10.1016/j.joei.2017.05.009

Chen, R., Lu, S., Zhang, Y., & Lo, S. (2017). Pyrolysis study of waste cable hose with thermogravimetry/Fourier transform infrared/mass spectrometry analysis. *Energy Conversion and Management, 153*, 83-92. doi:10.1016/j.enconman.2017.09.071

Chen, Z., Hu, M., Zhu, X., Guo, D., Liu, S., Hu, Z., Xiao, B., Wang, J. & Laghari, M. (2015). Characteristics and kinetic study on pyrolysis of five lignocellulosic biomass via thermogravimetric analysis. *Bioresource Technology*, *192*, 441-450. doi: 10.1016/j.biortech.2015.05.062

Chew, J., Doshi, V., Yong, S., & Bhattacharya, S. (2016). Kinetic study of torrefaction of oil palm shell, mesocarp and empty fruit bunch. *Journal Of Thermal Analysis And Calorimetry*, *126*(2), 709-715. doi:10.1007/s10973-016-5518-3

da Silva, J., Alves, J., Galdino, W., Andersen, S., & de Sena, R. (2018). Pyrolysis kinetic evaluation by single-step for waste wood from reforestation. *Waste Management*, *72*, 265-273. doi:10.1016/j.wasman.2017.11.034

Dhyani, V., & Bhaskar, T. (2018). A comprehensive review on the pyrolysis of lignocellulosic biomass. *Renewable Energy*, *129*, 695-716. doi:10.1016/j.renene.2017.04.035

Faizal, H., Shamsuddin, H., Heiree, M., Hanaffi, M., Rahman, M.R., Rahman, M., & Latiff, Z. (2018). Torrefaction of densified mesocarp fibre and palm kernel shell. *Renewable Energy*, *122*, 419-428. doi:10.1016/j.renene.2018.01.118

Fedepalma. (2018). Con récord en producción de aceite de palma, sector palmero colombiano cierra 2017 con balance positivo. Retrieved from http://web.fedepalma.org/con-record-en-produccion-de-aceite-de-palma-sector-palmero-colombiano-cierra-2017-con-balance-positivo

Flynn, J. H., & Wall, L. A. (1966). General Treatment of the Thermogravimetry of Polymers. Journal of Research of the National Bureau of Standards, *70*(6), 487–523. doi:10.6028/jres.070A.044

Friedman, H. L. (1964). Kinetics of thermal degradation of char-forming plastics from thermogravimetry. Application to a phenolic plastic. *Journal of Polymer Science Part C: Polymer Symposia*, *6*(1), 183–195. doi: 10.1002/polc.5070060121

Hu, M., Chen, Z., Wang, S., Guo, D., Ma, C., Zhou, Y., Chen, J., Laghari, M., Fazal, S., Xiao, B., Zhang, B. & Ma, S. (2016). Thermogravimetric kinetics of lignocellulosic biomass slow pyrolysis using distributed activation energy model, Fraser–Suzuki deconvolution, and iso-conversional method. *Energy Conversion and Management*, *118*, 1-11. doi: 10.1016/j.enconman.2016.03.058

Jankovic, B. (2008). Kinetic analysis of the nonisothermal decomposition of potassium metabisulfite using the model-fitting and isoconversional (model-free) methods. *Chemical Engineering Journal*, *139*(1), 128-135. doi: 10.1016/j.cej.2007.07.085

Jeguirim, M., Bikai, J., Elmay, Y., Limousy, L. & Njeugna, E. (2014). Thermal characterization and pyrolysis kinetics of tropical biomass feedstocks for energy recovery. *Energy for Sustainable Development*, *23*, 188-193. doi: 10.1016/j.esd.2014.09.009

Jenkins, B., Baxter, L., Miles, T., & Miles, T. (1998). Combustion properties of biomass. *Fuel Processing Technology*, *54*(1-3), 17-46. doi: 10.1016/s0378-3820(97)00059-3

Knežević, D. (2009). Hydrothermal conversion of biomass. (tesis de doctorado) University of Twente, Paises Bajos, p.11.

Kong, S., Loh, S., Bachmann, R., Rahim, S., & Salimon, J. (2014). Biochar from oil palm biomass: A review of its potential and challenges. *Renewable And Sustainable Energy Reviews*, *39*, 729-739. doi: 10.1016/j.rser.2014.07.107

Kongkaew, N., Pruksakit, W., & Patumsawad, S. (2015). Thermogravimetric Kinetic Analysis of the Pyrolysis of Rice Straw. Energy Procedia, *79*, 663-670. doi: 10.1016/j.egypro.2015.11.552

Lee, X., Lee, L., Gan, S., Thangalazhy-Gopakumar, S., & Ng, H. (2017). Biochar potential evaluation of palm oil wastes through slow pyrolysis: Thermochemical characterization and pyrolytic kinetic studies. *Bioresource Technology*, *236*, 155-163. doi: 10.1016/j.biortech.2017.03.105

Liu, Q., Zhong, Z., Wang, S. & Luo, Z. (2011). Interactions of biomass components during pyrolysis: A TG-FTIR study. *Journal of Analytical and Applied Pyrolysis*, *90*(2), 213-218. doi:10.1016/j.jaap.2010.12.009

Mishra, G., & Bhaskar, T. (2014). Non isothermal model free kinetics for pyrolysis of rice straw. *Bioresource Technology*, *169*, 614-621. doi:10.1016/j.biortech.2014.07.045

Mishra, R. & Mohanty, K. (2018). Pyrolysis kinetics and thermal behavior of waste sawdust biomass using thermogravimetric analysis. *Bioresource Technology*, *251*, 63-74. doi: 10.1016/j.biortech.2017.12.029

Monir, M., Abd Aziz, A., Kristanti, R., & Yousuf, A. (2018). Co-gasification of empty fruit bunch in a downdraft reactor: A pilot scale approach. *Bioresource Technology Reports*, *1*, 39-49. doi: 10.1016/j.biteb.2018.02.001

Nyakuma, B., Ahmad, A., Abdullah, T., Oladokun, O., & Aminu, D. (2015). Non-Isothermal Kinetic Analysis of Oil Palm Empty Fruit Bunch Pellets by Thermogravimetric Analysis. *Chemical Engineering Transactions, 45*, 1327-1332. doi: 10.3303/CET1545222

Oliva Domínguez, J., (2003). *Efectos de los productos de degradación originados en la explosión por vapor de biomasa de chopo sobre Kluyveromyces marxianus*. (tesis doctoral). Universidad Complutense de Madrid. Recuperado de: http://biblioteca.ucm.es/tesis/bio/ucm-t26833.pdf

Ozawa, T. (1965). A new method of analizing thermogravimetric data. *Bulletin of the chemical Society of Japan, 38*(11),1881–1886. doi:10.1246/bcsj.38.1881.

Parikh, J., Channiwala, S., & Ghosal, G. (2007). A correlation for calculating elemental composition from proximate analysis of biomass materials. *Fuel*, *86*(12-13), 1710-1719. doi:10.1016/j.fuel.2006.12.029

Peel, M., Finlayson, B., & McMahon, T. (2007). Updated world map of the Köppen-Geiger climate classification. *Hydrology and Earth System Sciences Discussions*, *4*(2), 439-473. doi:10.5194/hess-11-1633-2007

Pérez-Maqueda, L., & Criado, J. (2000). Journal Of Thermal Analysis And Calorimetry, *60*(3), 909-915. doi: 10.1023/a:1010115926340

Quan, C., Gao, N., & Song, Q. (2016). Pyrolysis of biomass components in a TGA and a fixed-bed reactor: Thermochemical behaviors, kinetics, and product characterization. Journal of Analytical and Applied Pyrolysis, *121*, 84-92. doi: 10.1016/j.jaap.2016.07.005

Rueda-Ordóñez, Y., & Tannous, K. (2015). Isoconversional kinetic study of the thermal

decomposition of sugarcane straw for thermal conversion processes. *Bioresource Technology*, *196*, 136-144. doi:10.1016/j.biortech.2015.07.062

Rueda-Ordóñez, Y., & Tannous, K. (2018). Drying and thermal decomposition kinetics of sugarcane straw by nonisothermal thermogravimetric analysis. *Bioresource Technology*, *264*, 131-139. doi: 10.1016/j.biortech.2018.04.064

Rueda-Ordóñez, Y., Tannous, K., & Olivares-Gómez, E. (2015). An empirical model to obtain the kinetic parameters of lignocellulosic biomass pyrolysis in an independent parallel reactions scheme. *Fuel Processing Technology*, *140*, 222-230. doi: 10.1016/j.fuproc.2015.09.001

Rueda-Ordóñez, Y.J., Baroni, E.G., Tinoco-Navarro, L.K., Tannous, K. (2015). Modeling the kinetics of lignocellulosic biomass pyrolysis. In: Tannous, K. (Ed.), Innovative Solutions in Fluid-Particle Systems and Renewable Energy Management. IGI Global, Hershey, 92–130. doi:10.4018/978-1-4666-8711-0.ch004.

Santos, K., Lobato, F., Lira, T., Murata, V., & Barrozo, M. (2010). Diferential evolution method applied to kinetic parameters estimation of bagasse pyrolysis. *Asociación Argentina De Mecánica Computacional*, 2535-2548.

Santos, K., Lobato, F., Lira, T., Murata, V., & Barrozo, M. (2012). Sensitivity analysis applied to independent parallel reaction model for pyrolysis of bagasse. *Chemical Engineering Research And Design*, *90*(11), 1989-1996. doi: 10.1016/j.cherd.2012.04.007

Sfakiotakis, S., & Vamvuka, D. (2015). Development of a modified independent parallel reactions kinetic model and comparison with the distributed activation energy model for the pyrolysis of a wide variety of biomass fuels. *Bioresource Technology*, *197*, 434-442. doi: 10.1016/j.biortech.2015.08.130

Sukiran, M., Abnisa, F., Daud, W., Bakar, N., & Loh, S. (2017). A review of torrefaction of oil palm solid wastes for biofuel production. *Energy Conversion And Management*, *149*, 101-120. doi: 10.1016/j.enconman.2017.07.011

Van Dam, J. (2016). Subproductos de la palma de aceite como materias primas de biomasa. *Palmas*, *37*(Especial Tomo II), 149-156.

Van Krevelen, D., Van Heerden, C., & Huntjens, F. (1951). Physicochemical aspects of the pyrolysis of coal and related organic compounds. *Fuel*, *30*, 253–259

Vyazovkin**,** S. (2000). Modification of the integral isoconversional method to account for variation in the activation energy. *Journal of Computational Chemistry*, *22*(2), 178-183. doi: 10.1002/1096-987X(20010130)22:2<178::AID-JCC5>3.0.CO;2-#

Vyazovkin, S., Burnham, A., Criado, J., Pérez-Maqueda, L., Popescu, C., & Sbirrazzuoli, N. (2011). ICTAC Kinetics Committee recommendations for performing kinetic computations on thermal analysis data. Thermochimica Acta, *520*(1-2), 1-19. doi: 10.1016/j.tca.2011.03.034

Wadhwani, R., Sutherland, D., Moinuddin, K. & Joseph, P. (2017). Kinetics of pyrolysis of litter materials from pine and eucalyptus forests. *Journal of Thermal Analysis and Calorimetry*, *130*(3), 2035-2046. doi.org/10.1007/s10973-017-6512-0

Wróblewski, R., & Ceran, B. (2016). Thermogravimetric analysis in the study of solid fuels. *E3S Web Of Conferences*, *10*(00109). doi: 10.1051/e3sconf/20161000109

Xiang, Z., Liang, J., Morgan Jr., H.M., Liu, Y., Mao, H., & Bu, Q. (2018). Thermal behavior and kinetic study for co-pyrolysis of lignocellulosic biomass with polyethylene over Cobalt

modified ZSM-5 catalyst by thermogravimetric analysis. *Bioresource. Technology*. *247*, 804-811. doi: 10.1016/j.biortech.2017.09.178

Yu, H., Liu, F., Ke, M., & Zhang, X. (2015). Thermogravimetric analysis and kinetic study of bamboo waste treated by Echinodontium taxodii using a modified three-parallel-reactions model. *Bioresource Technology*, *185*, 324-330. doi: 10.1016/j.biortech.2015.03.005